PCCP

Accepted Manuscript

ROYAL SOCIETY OF CHEMISTRY

www.rsc.org/pccp

PCCP

PAPER

Self-diffusion, Velocity Cross-correlation, Distinct Diffusion and Resistance Coefficients of the Ionic Liquid [BMIM][Tf_2N] at High Pressure†

Received 00th January 20xx,
Accepted 00th January 20xx

DOI: 10.1039/x0xx00000x

www.rsc.org/

Kenneth R. Harris[a] and Mitsuhiro Kanakubo[b]

Ion self-diffusion coefficients (D_{si}) have been measured for the ionic liquid 1-butyl-3-methylimidazolium bis(trifluoromethanesulfonyl)amide [BMIM][Tf_2N] at pressures to 200 MPa between 25 and 75 °C and at 0.1 MPa between 10 and 90 °C. Self-diffusion coefficients are reported for 1-ethyl-, 1-hexyl- and 1-octyl-3-methylimidazolium bis(trifluoromethanesulfonyl)amide salts at 0.1 MPa, supplemented by viscosity, electrical conductivity and density measurements. Velocity cross-correlation (VCC, f_{ij}) and distinct diffusion coefficients (D^d_{ij}) are calculated from the data. Both D_{si} and D^d_{ij} are analysed in terms of (fractional) Stokes-Einstein-Sutherland (SES) equations. SES and Walden plots show almost identical slopes, with high-pressure isotherms and the atmospheric pressure isobar falling on common, single lines for each property for [BMIM][Tf_2N]. SES plots for the anion self-diffusion coefficients for the [RMIM][Tf_2N] (R = alkyl) series are coincident, whereas those for the cations depend on their alkyl substitution, as do the Walden plots. In common with other [Tf_2N]- salts, the VCC follow the order $f_{--} < f_{++} < f_{+-}$. The Nernst-Einstein deviation parameter Δ for [BMIM][Tf_2N] is independent of temperature and pressure. Those for the other [Tf_2N]- salts are independent of temperature. Δ increases in magnitude with increasing alkyl chain length on the cation. The transport properties of [BMIM][Tf_2N] are re-examined in terms of density scaling using reduced conductivities and reduced molar conductivities for the first time. Identical scaling parameters (γ) are obtained for the several reduced transport properties. This result is supported by data for other ionic liquids. It is suggested that the γ for ionic liquids may depend on packing fraction.

Introduction

We have made several studies of the transport properties of ionic liquids at high pressure, including the viscosity, ion self-diffusion coefficients and electrical conductivity.[1,2,3,4] Here we extend this work by reporting ion self-diffusion coefficients for the ionic liquid 1-butyl-3-methylimidazolium bis(trifluoromethanesulfonyl)amide, [BMIM][Tf_2N], at high pressure between 25 and 75 °C, supplemented by atmospheric pressure data between 10 and 90 °C. This common imidazolium salt is an important reference material for ionic liquid studies, being more stable than its $[BF_4]^-$ and $[PF_6]^-$ analogues, which can slowly hydrolyse at moderate temperatures in the presence of traces of water. This report completes a sequence of measurements, including the density,[5] viscosity[6] and electrical conductivity[7] for [BMIM][Tf_2N] under high pressure. This then permits analysis in terms of the scaling of the self-diffusion coefficients (Stokes-Einstein-Sutherland) and the molar conductivity (Walden), together with the derived distinct diffusion coefficients, DDC or D^d_{ij} (i,j = +,-),[8] for like ion (cation-cation and anion-anion) and unlike ion (cation-anion) interactions (Stokes-Einstein-Sutherland), with the viscosity. We also report (Laity) resistance coefficients, r_{ij}, and re-examine thermodynamic (density) scaling for this substance.[9]

For comparison of trends within the 1-alkyl-3-methylimidazolium bis(trifluoromethanesulfonyl)amide series, self-diffusion coefficients are also reported for the 1-ethyl-, 1-hexyl- and 1-octyl-3-methylimidazolium bis(trifluoromethanesulfonyl)amide salts at atmospheric pressure. New density, conductivity and viscosity data for [BMIM][Tf_2N], [HMIM][Tf_2N] and [OMIM][Tf_2N] at atmospheric pressure are included. The density, conductivity and viscosity measurements for [BMIM][Tf_2N] and [HMIM][Tf_2N] extend to sub-zero temperatures, supplementing previous measurements.[5,6,7]

Our earlier high-pressure work, on other imidazolium salts[1,2,4] and a single pyrollidinium salt,[3] has shown that the self-diffusion coefficients (D_i) and the molar conductivity (Λ) depend on the viscosity (η) in a regular way, such that the slopes of Stokes-Einstein-Sutherland plots for the self-diffusion coefficients and that of a Walden plot have, for a given ionic liquid, very similar, if not identical, fractional slopes. Both self-

[a] School of Physical, Environmental and Mathematical Sciences, University College, University of New South Wales, PO Box 7916, Canberra BC, ACT 2610, Australia. E-mail: k.harris@adfa.edu.au
[b] National Institute of Advanced Industrial Science and Technology (AIST), 4-2-1 Nigatake, Miyagino-ku, Sendai 983-8551, Japan. E-mail: m-kanakubo@aist.go.jp

† Electronic Supplementary Information (ESI) available: Numerical tables of experimental diffusion coefficients as a function of temperature and pressure, experimental densities, conductivities and viscosities, derived expansivities, velocity correlation, distinct diffusion, and resistance coefficients, and Nernst–Einstein deviation parameters. See DOI: 10.1039/x0xx00000x

diffusion coefficients and the molar conductivity are functionals of Kubo velocity correlation functions and therefore can be used to calculate both time and ensemble averaged velocity cross-correlation coefficients f_{ij} (i,j = +,-), for like ion (cation-cation and anion-anion) and unlike ion (cation-anion) interactions:[10]

$$f_{++} \equiv \frac{N_A V}{3}\int_0^\infty \left\langle \mathbf{v}_{+\alpha}(0)\cdot\mathbf{v}_{+\beta}(t)\right\rangle \mathrm{d}t = RT\kappa\left(\frac{M_-}{z_- FcM}\right)^2 - \frac{D_+}{\nu_+ c} \quad (1)$$

(with an analogous form for anion-anion velocity correlations, f_{--}), and

$$f_{+-} \equiv \frac{N_A V}{3}\int_0^\infty \left\langle \mathbf{v}_{+\alpha}(0)\cdot\mathbf{v}_{-\beta}(t)\right\rangle \mathrm{d}t = RT\kappa\frac{M_+ M_-}{z_+ z_- (FcM)^2} \quad (2)$$

(where N_A is the Avogadro constant, F the Faraday, V the volume of the ensemble, κ is the conductivity, c the amount concentration (molarity) of salt, t time, $\mathbf{v}_i$ are ion velocities, z_i and ν_i are (signed) charge and stoichiometric numbers, and M, M_+, and M_- are the molar masses of salt, cation, and anion, respectively). Note that the f_{ij} are negative quantities for a pure salt.[10] The VCC, in the form of distinct diffusion coefficients,

$$D_{ij}^d = cf_{ij}(\nu_+ + \nu_-) = \nu c f_{ij} \quad (3)$$

also show similar fractional slopes when plotted in the Stokes-Einstein-Sutherland and Walden forms.[4,11] In both these plots, whether of the experimentally measured transport coefficients or the distinct diffusion coefficients, data points for a given ionic liquid on high pressure isotherms fall on the same line as points on the atmospheric pressure isobar for the substances examined thus far.[1-4] The conclusion is that those transport properties that are functionals of Kubo velocity correlation functions (D_i and Λ) scale with the viscosity, not temperature, pressure or density per se.

The Nernst-Einstein (NE) equation can be used to relate conductivities with ion self-diffusion coefficients.

$$\Lambda = \left(F^2/RT\right)\left(\nu_+ z_+^{\,2} D_+ + \nu_- z_-^{\,2} D_-\right)(1-\Delta) \quad (4)$$

The NE deviation parameter Δ is zero at infinite dilution in electrolyte solutions where the ions cannot interact and eqn (4) is then a form of the well-known Nernst-Hartley equation relating limiting conductivities, self-diffusion coefficients and the limiting mutual diffusion coefficient.[12,13] In a single component molten salt Δ is always positive, except in the case of ''super-ionicity''[4]. It can be expressed directly in terms of the velocity cross-correlation coefficients (VCC or f_{ij}) for like-ion and unlike-ion interactions.[11] Thus

$$\begin{aligned}\Delta &= -\frac{c\left(2\nu_+\nu_- z_+ z_- f_{+-} + \nu_+^2 z_+^2 f_{++} + \nu_-^2 z_-^2 f_{--}\right)}{\left(\nu_+ z_+^2 D_+ + \nu_- z_-^2 D_-\right)} \\ &= \frac{2c[\,f_{+-} - (f_{++}+f_{--})/2]}{(D_+/\nu_+ + D_-/\nu_-)} \\ &= \frac{2[D_{+-}^d - (D_{++}^d + D_{--}^d)/2]}{\nu(D_+/\nu_+ + D_-/\nu_-)}\end{aligned} \quad (5)$$

$\Delta = 0$ can then only result for the arbitrary condition that

$$\begin{aligned} f_{+-} &= (f_{++} + f_{--})/2 \\ &\text{or} \\ D_{+-}^d &= (D_{++}^d + D_{--}^d)/2 \end{aligned} \quad (6)$$

In all cases studied, (the f_{ij} and D^d_{ij} being negative quantities), f_{+-} is greater (i.e. smaller in magnitude) than the arithmetic mean of f_{++} and f_{--}.

An equivalent description, in terms of irreversible thermodynamics, can be made using resistance coefficients. For molten salts, the most convenient formalism[13] is that of Laity:[14,15]

$$X_i \equiv -(\mathrm{grad}\,\mu_i)_T = \sum_{k=1}^{N} r_{ik} x_k (\mathbf{v}_i - \mathbf{v}_k) \quad (7)$$

where X_i is the thermodynamic or generalised frictional force on ion species i in an electrochemical potential (μ_i) gradient, x_k is the mole fraction, ($\mathbf{v}_i$ - $\mathbf{v}_k$) is the velocity of species i relative to that of species k, and the r_{ik} are the resistance coefficients. Due to the theorem of Onsager,[13,16] the reciprocity relation, r_{ik} = r_{ki} holds. For a one component system with two ionic species,[14]

$$r_{+-} = z_+\nu_+(z_+ + |z_-|)F^2/\Lambda \quad (8)$$

and

$$r_{ii} = \frac{1}{|z_j|}\left[\frac{(z_+ + z_-)RT}{D_i} - |z_i| r_{+-}\right], \quad i = +,-; \quad j \neq i \quad (9)$$

r_{+-} is necessarily positive, but the two r_{ii} may be positive or negative. The condition equivalent to eqn (6), giving $\Delta = 0$, is

$$r_{+-}^2 = r_{++} r_{--} \quad (10)$$

i.e. r_{+-} is the geometric mean of the cation and anion resistance coefficients.[17] Generally, ${r_{+-}}^2 > (r_{++}\, r_{--})$, corresponding to $f_{+-} > (f_{++} + f_{--})/2$. Here we calculate and examine resistance coefficients of an ionic liquid for the first time.

It is now commonplace to use thermodynamic or density scaling in fitting liquid transport property data to functionals of the group (TV^γ) where the scaling parameter γ is a constant for a given property. This requires high pressure data and there is now an extensive literature on the subject.[9,18,19] For particles interacting through an effective inverse power law,

$$U(r) = \varepsilon(\sigma/r)^n \quad (11)$$

and then $\gamma = n/3$. While ionic liquids interacting through both attractive and repulsive Coulombic forces may not fit the definition of a "Roskilde-simple liquid"[20] where the potential energies of particle configurations are scaled uniformly to a different density, and interactions at the high densities obtaining in liquids are primarily repulsive, scaling is nevertheless found to apply. Clearly the particle dynamics are similarly governed by the dense liquid structure, though much

smaller values of γ (1 - 3.5) obtain than for molecular liquids (> 7).[9] This is consistent with $n = 1$ for the one-component plasma fluid model.[21]

It has been argued that it is reduced forms of the transport properties that should be scaled[22,23] using dimensionless expressions suggested by kinetic theory,[24,25] with scaling being made in terms of the mean inter-particle distance, $d = v^{1/3}$ [where v is the molecular volume (V_m/N_A)], and the thermal velocity, $v_{th} = \sqrt{(k_BT/m)}$, [where m is the molecular mass (M/N_A), M being the molar mass]. This type of scaling differs from others in that macroscopic parameters (m, T,V) are used in place of the inter-particle potential parameters, (σ, ε), as in the van der Waals hard-sphere comparison approach and its modifications.[26,27,28] For the viscosity, η, thermal conductivity, λ, and self-diffusion coefficient, D_{Si}, the appropriate expressions are:

$$\eta^* = \eta v^{2/3}/\sqrt{mk_BT} \tag{12}$$

$$\lambda^* = \frac{\lambda v^{2/3}}{k_B\sqrt{(k_BT/m)}} \tag{13}$$

$$D_{Si}^* = D_{Si} v^{-1/3}\sqrt{m/k_BT} \tag{14}$$

Strictly speaking, for salts, with two ionic species, the reduced mass, $\mu = (1/m_+ + 1/m_-)^{-1}$, should be employed, but this makes no practical difference to the determination of γ. Fragiadakis and Roland[23] showed that this procedure gives values of γ_D and γ_η much closer to one another for molecular liquids, the former being increased and the latter decreased, relative to the fits for the unreduced properties. This behaviour was confirmed by López et al.[9] for ionic liquids and is consistent with the idea of "quasi-universality", that is, that "simple" liquid systems "have very similar physics as regards structure and dynamics."[21]

Here we extend this approach, suggesting the following forms for the reduced conductivity and molar conductivity:

$$\kappa^* = \kappa\sqrt{(mk_BT)}[e^2v^{-2/3}] \tag{15}$$

$$\Lambda^* = \Lambda\sqrt{(mk_BT)}N_A/[e^2v^{1/3}] \tag{16}$$

where e is the electronic charge. The scaling parameters for these two quantities are compared with the values obtained for the reduced viscosity and self-diffusion coefficients, both for [BMIM][Tf_2N] and the other ionic liquids for which there are high pressure data.

Table 1 Substances and water content.

Substance	CAS no	M/g·mol^{-1}	10^6 wt fraction H_2O
[EMIM][Tf_2N]	174899-82-2	391.31	30
[BMIM][Tf_2N]	174899-83-3	419.36	20
[HMIM][Tf_2N]	382150-50-7	447.42	20
[OMIM][Tf_2N]	178631-04-4	475.47	20

Experimental

The preparation of the sample materials was described in the papers on the density, viscosity and conductivity.[5-7] The samples were prepared in Sendai, and aliquots sealed in evacuated 5 mm NMR tubes for the atmospheric pressure diffusion measurements in Canberra. The samples for the high-pressure self-diffusion measurements and atmospheric pressure densities were sealed in evacuated glass ampoules until use. Such dry and out-gassed samples have been found to be stable for five years and more. The Teflon high-pressure diffusion cell was loaded in a dry box prior to insertion in the pressure vessel. The molar masses and water content are given in Table 1.

The steady-gradient spin-echo NMR self-diffusion apparatus and its calibration and application to ionic liquids have been described in previous work.[1-4] As is usual for ionic liquids, the temperature range that could be covered by our apparatus was limited by the short T_2 relaxation times, which attenuate the signal in addition to diffusion, with greater effect at lower temperatures, giving low signal to noise ratios. The high pressure isotherms were normalised on the atmospheric pressure results to remove any calibration difference between the low and high pressure magnetic field gradient coils (the latter is contained within the pressure vessel). The estimated relative standard uncertainty in D is 3% and 0.05 K in the temperature.

Atmospheric pressure densities for [OMIM][Tf_2N] were determined between (0 and 90) °C with an Anton Paar DMA5000 vibrating tube densimeter as described previously. From a comparison of results for three samples of [HMIM][Tf_2N] with two different instruments, the relative standard uncertainty is estimated at 0.02%.[5] The standard uncertainty in the temperature was 0.01 K.

For [BMIM][Tf_2N] and [HMIM][Tf_2N], our earlier density measurements[5,6] were extended to -35 °C using the vibrating tube densimeter built into the Stabinger rotating cylinder viscometer described below. The relative standard uncertainty is estimated at 0.04%, this level of agreement being attained with the DMA5000 results for [BMIM][Tf_2N]; for [HMIM][Tf_2N] the agreement was 0.02%. The standard uncertainty in the temperature is 0.02 K between (15 and 105) °C and 0.05 K below 15 °C.

Electrical conductivities at atmospheric pressure were measured by electrochemical impedance spectroscopy using an impedance analyzer (Bio Logic potentiostat/galvanostat, model SP-150), the sample resistance being determined from a Nyquist plot over the frequency range 0.1 Hz ~ 1 MHz.7, [29] The glass cell had bright platinum electrodes. Potentiostatic and galvanostatic measurements yielded the same results within experimental uncertainty, estimated at 2%. This method is superior[7] to the conductance bridge method used previously.[1,2,30] The standard uncertainty in the temperature was 0.01 K.

Viscosities for [HMIM][Tf_2N] were determined with a falling body viscometer as in previous work.[6] The relative expanded uncertainty is 2%. The standard uncertainty in the temperature is 0.01 K. Viscosities at atmospheric pressure for

Table 2 Coefficients of the polynomial $\rho = a_0 + a_1 T + a_2 T^2$ for the density of [EMIM][Tf_2N], [BMIM][Tf_2N], [HMIM][Tf_2N] and [OMIM][Tf_2N] at 0.1 MPa[a]

	a_0 /g·cm^{-3}	$10^3\,a_1$ /g·cm^{-3}·K^{-1}	$10^6 a_2$ /g·cm^{-3}·K^{-2}	$u_r(\rho)$ [b] /μg·cm^{-3}
[EMIM][Tf_2N][37]	1.859 12	-1.266 8	0.4230	100
(0 – 90) °C	(0.000 9)	(0.005)	(0.079)	
[BMIM][Tf_2N]	1.764 46	-1.242 2	0.4718	100
(-30 – 90) °C	(0.0018)	(0.012)	(0.020)	
[HMIM][Tf_2N]	1.688 50	-1.197 2	0.4553	180
(-35 – 90) °C	(0.0028)	(0.019)	(0.032)	
[OMIM][Tf_2N]	1.611 52	-1.061 8	0.2891	70
(0 - 90) °C	(0.0022)	(0.014)	(0.023)	

[a] Units: T/K, ρ/g·cm^{-3}.The standard uncertainties of the fitted coefficients are given in parentheses. [b] u_r, relative standard uncertainty of the fit. The values for [EMIM][Tf_2N] from ref. 37 are included for comparison.

[BMIM][Tf_2N], [HMIM][Tf_2N] (supplementing and extending the falling body results to lower temperatures) and [OMIM][Tf_2N] were determined with an Anton Paar Stabinger SVM 3000 rotating-cylinder viscometer, calibrated using S60, N100, S200 and N2500 reference fluids supplied by the Cannon Instrument Company. The estimated standard uncertainty is 2%.[29] The standard uncertainty in the temperature is 0.02 K between (15 and 105) °C and 0.05 K below 15 °C. Temperatures below 0°C were obtained using an external Julabo FP50 thermostat for both viscometry and conductivity measurements.

Results

Densities for [OMIM][Tf_2N] at atmospheric pressure are given in Table S1 of the Supplementary Information. They were fitted to a polynomial in the temperature: the fitted coefficients and relative standard uncertainties are listed in Table 2. Fig. 1 compares literature data[31,32,33,34,35] with our results. The values of Jacquemin et al.[34] are in good agreement with those of this work (-0.04%), but those of Yunus et al.[35] are significantly higher by 0.5%, whereas those of Tariq et al.[32] and of Kolbeck et al.[33] are 0.13% and a large 0.75% lower, respectively. The results of Gardas et al.[31] intersect ours, but have too steep a temperature dependence. The derived expansivities (Table S1), obtained between by differentiation of the polynomial density fits, are independent of temperature between (0 and 90 °C), with an average value of (0.674 ± 0.015)·10^{-3} K^{-1}. [The standard uncertainty (k = 1) is derived from those for the coefficients obtained for the polynomial fit to the density.] We have obtained very similar values for both [BMIM][Tf_2N] and [HMIM][Tf_2N], [(0.666 ± 0.02) and (0.666 ± 0.02)·10^{-3} K^{-1}, respectively, in previous work.[5,6,36] A value of (0.666 ± 0.007) ·10^{-3} K^{-1} can be derived from previous results for [EMIM][Tf_2N] from the Sendai laboratory.[37]

The Stabinger density results for [BMIM][Tf_2N] and [HMIM][Tf_2N], which extend to -30 and -35 °C, respectively, in the supercooled region, are also given in Table S1 and summarised in Table 2. The expansivities show a small, negative temperature dependence: the mean values, (0. 670 ± 0.012)·10^{-3} K^{-1} and (0.676 ± 0.02)·10^{-3} K^{-1}, are consistent with the values above.

Electrical (κ) and molar conductivities (Λ) at atmospheric pressure for [HMIM][Tf_2N] and [OMIM][Tf_2N] are given in Table S2. Data for [EMIM][Tf_2N][37] and [BMIM][Tf_2N][7] from the Sendai laboratory have been published previously, but those for [BMIM][Tf_2N] have now been extended to -30 °C and the new points are also given in Table S2.

The conductivities and molar conductivities were fitted to the standard Vogel-Fulcher-Tammann (VFT) equation generally employed for IL transport properties:

$$\kappa, \Lambda, \eta, D_i = \exp(A + B/(T - T_0)) \qquad (17)$$

The coefficients are given in Table 3. Comparison with the literature for [BMIM][Tf_2N] at temperatures above 0 °C has been made recently:[7] the extension to lower temperatures in this work does not improve the comparison with the conductivities derived from broadband dielectric spectroscopic measurements by Wojnarowska et al.[38] which are higher by a factor of 3 to 4 in the range 220-230 K than values extrapolated from our lowest temperature of 243 K using eqn (17).

Fig. 2 compares literature data[39,40,41,42,43,44,45,46] for the conductivities (κ) of the [HMIM][Tf_2N] and [OMIM][Tf_2N] with our results, also in terms of deviations from eqn (17). For [HMIM][Tf_2N] [Fig. 2(a)], there is excellent agreement across the data sets except for the higher values of Tokuda et al.[40] at lower temperatures, and the systematically lower values of Rupp et al.[46] For [OMIM][Tf_2N], [Fig. 2(b)], there are repeated trends for the values of Tokuda et al.[40] and of Rupp et al.[46] in comparison to ours.

We note that the conductivities do not well fit the 2-parameter Litovitz equation which we have used in previous

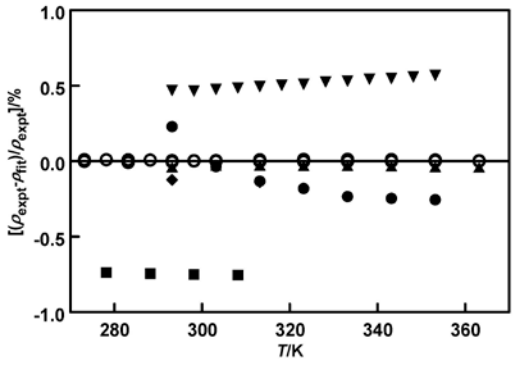

Fig. 1 Relative deviations for the fit of the atmospheric pressure densities (ρ) for [OMIM][Tf_2N] as a function of temperature: open circles, this work; filled circles, Gardas et al.,[31] DMA 60 VTD, [H_2O] 21 ppm, relative standard uncertainty u_r = 0.08%; solid diamonds, Tariq et al.,[32] DMA5000 VTD, [H_2O] 70 ppm, u_r = 0.02%; solid squares, Kolbeck et al.,[33] DMA5000 VTD, [H_2O] 78 ppm, u_r = 0.04%; solid triangles, Jacquemin et al.,[34] DMA512 VTD, [H_2O] 50 ppm, u_r = 0.04%; solid inverted triangles, Yunus et al.,[35] SVM 3000 Stabinger VTD, [H_2O] 146 ppm, u_r = 0.04%.

Table 3 Coefficients of Eqn 17 for the conductivities of [EMIM][Tf_2N],[BMIM][Tf_2N], [HMIM][Tf_2N] and [OMIM][Tf_2N] at 0.1 MPa[a,b]

	A	-*B*/K	T_0/K	$u_r(\kappa$ or $\Lambda)$/% [c]	*T* range/ °C
			[EMIM][Tf_2N][37]		
κ/ S·m^{-1}	4.040 (0.011)	538.8 (3.1)	167.7 (0. 4)	0.1	0 - 80
Λ/μS·m^2 ·mol^{-1}	9.788 (0.012)	578.6 (3.4)	164.5 (0.4)	0.1	
			[BMIM][Tf_2N]		
κ/S·m^{-1}	4.1824 (0.038)	661.09 (8.9)	168.481 (0.74)	1.2	-30 – 80
Λ/μS·m^2 ·mol^{-1}	10.0132 (0.036)	688.90 (8.5)	166.971 (0.69)	1.1	
			[HMIM][Tf_2N]		
κ/S·m^{-1}	4.3327 (0.040)	788.97 (9.4)	163.663 (0.68)	1.0	-30 – 80
Λ/μS·m^2 ·mol^{-1}	10.282 (0.036)	819.42 (8.6)	162.210 (0.61)	0.8	
			[OMIM][Tf_2N]		
κ/S·m^{-1}	4.1016 (0.031)	803.18 (8.5)	167.256 (0.71)	0.3	0 - 80
Λ/μS·m^2 ·mol^{-1}	10.1881 (0.029)	843.80 (8.1)	164.987 (0.66)	0.3	

[a] The standard uncertainties for the fitted coefficients are given in parentheses. The values for [EMIM][Tf_2N] from ref. 37 are included for comparison. [b] Strictly speaking it is illogical to fit both κ and Λ to eqn 17, as the density does not fit the VFT equation: nevertheless, as the temperature dependence of the density is very much less than that of κ, eqn 17 can be conveniently used for both quantities. [c] u_r, relative standard uncertainty of the fit.

Table 4 Coefficients of Eqn 17 for the viscosity of [EMIM][Tf_2N], [BMIM][Tf_2N], [HMIM][Tf_2N] and [OMIM][Tf_2N] at 0.1 MPa[a]

	[EMIM][Tf_2N]	[BMIM][Tf_2N]	[HMIM][Tf_2N]	[OMIM][Tf_2N]
	rotating cylinder[37]	Combined falling body[3] and rotating cylinder	Combined falling body and rotating cylinder	rotating cylinder
A	-1.494 (0.021)	-1.8644 (0.031)	-2.2869 (0.033)	-2.2187 (0.022)
B/K	694.8 (6.4)	781.77 (8.1)	909.24 (9.2)	919.33 (6.5)
T_0/K	159.0 (0.7)	163.50 (0.65)	159.21 (0.67)	162.103 (0.51)
u_r/% [b]		1.1 (0.8 FB, 1.5 RC)	1.2 (1.1 FB, 1.5 RC)	0.2
δ [c]	4.37	4.78	5.71	5.67
T_g (Angell eqn)/K	-	183.5	182.4	185.6
T_g (expt)/ K	-	181.5[60]	184.3[61]	185[62]
T range /°C	0 - 80	-20 – 90	-25 – 90	0 – 90

[a] The standard uncertainties for the fitted coefficients are given in parentheses. Viscosity units: mPa·s. The values for [EMIM][Tf_2N] from ref. 37 are included for comparison. [b] u_r, relative standard uncertainty of the fit. FB = falling body, RC = Stabinger rotating cylinder. [c] δ ($=B/T_0$) is the Angell strength factor; a lower δ indicates a more fragile liquid.

transport property studies:

$$\kappa, \Lambda = \exp(A' + B'/T^3) \quad (18)$$

This appears to be due simply to the extended temperature ranges of the new data compared to those of the earlier works and not to any "crossover" behaviour[4] as the 3-parameter VFT equation gives satisfactory fits over the whole temperature range.

Viscosities (η) at atmospheric pressure for [BMIM][Tf_2N] (rotating cylinder, -30 to 90 °C), [HMIM][Tf_2N] (rotating cylinder, -35 to 90 °C; falling body, 0 to 90 °C) and [OMIM][Tf_2N] (rotating cylinder, 0 to 90 °C) are given in Tables S3 and S4. (The same data for [HMIM][Tf_2N] have been used as part of a separate, concurrent study.[47]) Rotating-cylinder data for [EMIM][Tf_2N] from the Sendai laboratory[29] and falling-body [BMIM][Tf_2N] results from the Canberra laboratory[7] have been published previously. The coefficients for fits to the VFT equation (using combined falling body and rotating cylinder data sets for [BMIM][Tf_2N] and [HMIM][Tf_2N]) are given in Table 4. Again, Litovitz fits are poor for the extended temperature data sets.

Fig. 3 shows the fits to the VFT equation and a comparison with literature data.[32,34,48,49,50,51,52,53,54,55,56,57,58,59] For [BMIM][Tf_2N], our data from the rotating cylinder viscometer are systematically higher than those from the falling body instrument, though there is agreement within the total uncertainties. There is some distortion of the fit by the sub-zero rotating cylinder results and those below 253 K have been omitted from the fit. Overall, there is good agreement with the rotating cylinder viscometer results of Salgado et al.[52] and of Hiraga et al.,[54] the oscillating piston results of Atilhan et al.[51] and the falling ball results of Salinas et al.[58] The capillary viscometer results of Pan et al.,[48] the rotating cylinder results of Tariq et al.,[55] and the cone and plate viscosities of Vranes et al.[50] trend lower at lower temperatures.

For [HMIM][Tf_2N], our data lie slightly below the correlation from the 2009 IUPAC sponsored round-robin study[49] of a specific sample of [HMIM][Tf_2N] at lower temperatures and slightly above at high temperatures. There is good agreement with the capillary data of Santos et al.[44], despite the higher water content in their sample, and with the falling ball results of Salinas et al.[58] The rotating cylinder results of Tariq et al.[55] and of Iguchi et al.[57] agree well with one another and with our rotating cylinder data but all three sets trend higher than the correlation above 70 °C. The vibrating wire results of Diogo et al.[53] also trend higher with increasing temperature, but above 40 °C. The cone and plate data[45,50] agree near room temperature but deviate very strongly at lower and higher temperatures.

For [OMIM][Tf_2N] there is excellent agreement with the falling ball data of Almantariotis et al.,[59] fair agreement within the combined uncertainties with those of Tariq et al.,[55] and, again, very poor agreement above room temperature with the cone and plate results of Rupp et al.[46]

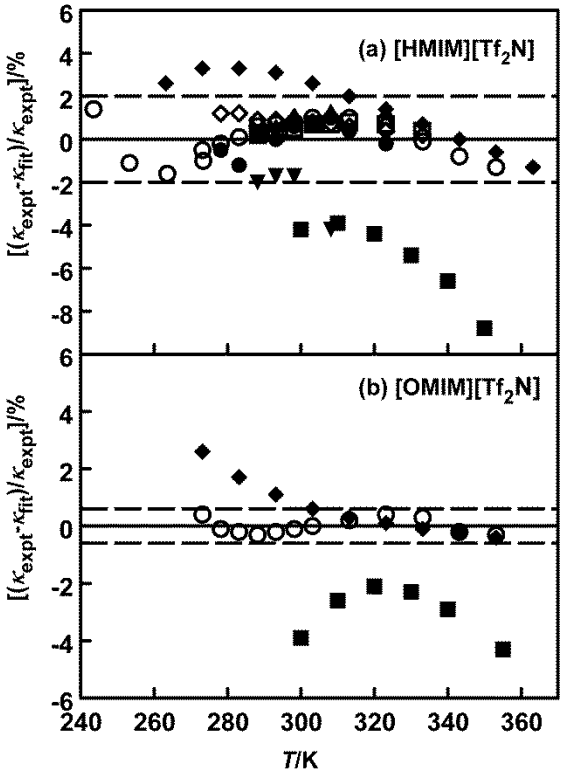

Fig. 2 Relative deviations for the fit of the atmospheric pressure conductivities (κ) to eqn (18) as a function of temperature. a) [HMIM][Tf_2N]: open circles, this work - the dotted lines show the relative expanded uncertainty of the fit to eqn (17) with a 95% confidence level (k = 2), U_r = 2%; open triangles, Widegren et al.,[39] impedance bridge, [H_2O] 10 ppm, relative standard uncertainty u_r = 2 %; solid diamonds, Tokuda et al.,[40] impedance analyser, [H_2O] < 10 ppm, u_r = 2 %; solid triangles, Widegren and Magee,[41] impedance bridge, [H_2O] 10 ppm, u_r = 2 %; solid circles, Kandil et al.,[42] impedance analyser, [H_2O] 90-180 ppm, u_r = 2 %; solid inverted triangles, Leys et al.,[43] dielectric spectroscopy, [H_2O] 66 ppm, precision not given; open diamonds, Santos et al.,[44] impedance analyser, [H_2O] 21-407 ppm, u_r = 2 %; open squares, Calado et al.,[45] lock-in amplifier impedance technique, [H_2O] 39-106 ppm, u_r = 2 %; solid squares, Rupp et al.,[46] conductance meter, [H_2O] < 20 ppm, precision not given. b) [OMIM][Tf_2N]: open circles, this work- the dotted lines show the expanded uncertainty of the fit to eqn (17) with a 95% confidence level (k = 2), U_r = 0.6 %; solid diamonds, Tokuda et al.,[40] impedance analyser, [H_2O] < 10 ppm, u_r = 2 %; solid squares, Rupp et al.,[46] conductance meter, [H_2O] < 20 ppm, uncertainty not given.

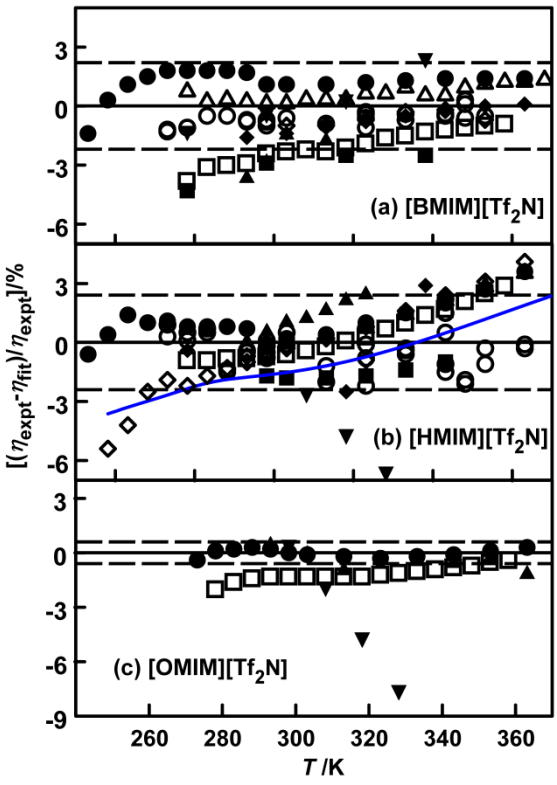

Fig. 3 Relative deviations for the fit of the atmospheric pressure viscosities (η) to eqn (17) as a function of temperature. a) [BMIM][Tf_2N]: open circles, falling body,[36] Canberra laboratory; closed circles, rotating cylinder, this work; the dotted lines show the expanded uncertainty of the VFT fit with a 95% confidence level (k = 2), U_r = 2.2%; filled squares, Pan et al.,[48] capillary, [H_2O] ~ 1 ppm, relative standard uncertainty u_r = 0.5%; open squares Tariq et al.,[55] rotating cylinder, [H_2O] < 70 ppm, u_r = 2 %; open diamonds, Atilhan et al.,[51] osc. piston, [H_2O] ~ 55 ppm, u_r = 2%; filled triangles, Vranes et al.,[50] cone and plate, [H_2O] ~ 100 ppm, ± 1%; open triangles, Salgado et al.,[52] rotating cylinder, [H_2O] < 150 ppm, u_r = 1%; inverted triangles, Salinas et al.,[58] falling ball, [H_2O] < 50 ppm, u_r = 0.5 %; filled diamonds, Hiraga et al.,[54] rotating cylinder, [H_2O] < 70 ppm, u_r = 0.35 %. b) [HMIM][Tf_2N]: open circles, falling body, this work; closed circles, rotating cylinder, this work; the dotted lines show the expanded uncertainty of the VFT fit with a 95% confidence level (k = 2), U_r = 2.4%; blue line, 2009 IUPAC correlation;[49] closed squares, Santos et al.,[44] capillary, [H_2O] 119-196 ppm, relative standard uncertainty u_r = 2.1 %; open squares, Tariq et al.,[55] rotating cylinder, [H_2O] < 70 ppm, u_r = 2 %; open diamond, Ahosseini et al.,[56] cone and plate, [H_2O] < 50 ppm, u_r = 1.2 %; solid triangles, Diogo et al,[53] vibrating wire, [H_2O] 25-89 ppm, u_r = 2 %; open triangles, Iguchi et al.,[57] rotating cylinder, [H_2O] ~20 ppm, u_r = 0.9 %; solid inverted triangles, Rupp et al.,[46] cone and plate, [H_2O] < 20 ppm, precision not given; solid diamonds, Salinas et al.,[58] falling ball, [H_2O] < 50 ppm, u_r = 0.5%.c) [OMIM][Tf_2N]: closed circles, rotating cylinder, this work; the dotted lines show the expanded uncertainty of the VFT fit with a 95% confidence level (k = 2), U_r = 0.6 %; open squares, Tariq et al.,[55] rotating cylinder, [H_2O] < 70 ppm, u_r = 2 %; solid triangles, Almantariotis et al,[59] falling ball, [H_2O] ~ 110 ppm, u_r = 1.5 %; solid inverted triangles, Rupp et al.,[46] cone and plate, [H_2O] < 20 ppm, precision not given.

One can predict glass temperatures, T_g, from the VFT equation parameters using the relationship of Angell, which we have employed in previous work.[3,6,36] In each case, there is good agreement with experimental values from the literature (Table 4).

Diogo et al.[63] have reviewed viscometry techniques as they are currently applied to ionic liquids due to the disparate results found in the literature even for well characterised samples. Calibration and cross-checking with suitable reference materials are not always adequately done. This review followed the IUPAC sponsored round-robin study[49] and subsequent work with a vibrating tube viscometer on a similar sample by Diogo et al.[53] In the review, Diogo et al.[63] raised questions about the applicability of the Stabinger rotating cylinder viscometer to ionic liquid measurements: in their words, "*However, to the authors' knowledge there has been no study of the effect of electromagnetic phenomena in the case when an electrically conducting liquid fills the annulus between the rotating tube and the inner rotor. At the very least, one could expect an investigation to demonstrate that the effect is negligible or non-existent. Its absence leaves unanswered questions about the*

validity of the method." We believe the good agreement between the results of this work for the falling body viscometer, which has well-developed working equations (see Harris et al.[64] and citations therein), and the rotating cylinder viscometer for both [BMIM][Tf_2N] and [HMIM]Tf_2N] in the region of overlapping temperatures taken together with earlier results for *N*-butyl-*N*-methylpyrrolidinium bis(trifluoromethylsulfonyl)-amide, [Pyr_{14}][Tf_2N],[3] at least partially answers these concerns, though we note that the rotating cylinder results tend to be slightly higher than the falling body ones and the rotating cylinder results did not well fit the VFT equation at the lowest temperatures, perhaps because these liquids were supercooled. Both viscometers are calibrated with high viscosity reference fluids as described in the experimental section and in earlier studies, but these are non-ionic.[3,36,64] Further work will be required to satisfactorily resolve this question.

The measured self-diffusion coefficients (D_{Si}) for both atmospheric and higher pressures for [BMIM][Tf_2N] are given in Table S5. Atmospheric pressure values for [EMIM][Tf_2N], [HMIM][Tf_2N] and [OMIM][Tf_2N] are given in Table S6. The atmospheric pressure D_{Si} values were also fitted to eqn (17) to allow comparison with literature data. The full data sets for [BMIM][Tf_2N] were fitted to the modified VFT equation (MVFT1, with T_0 independent of p:

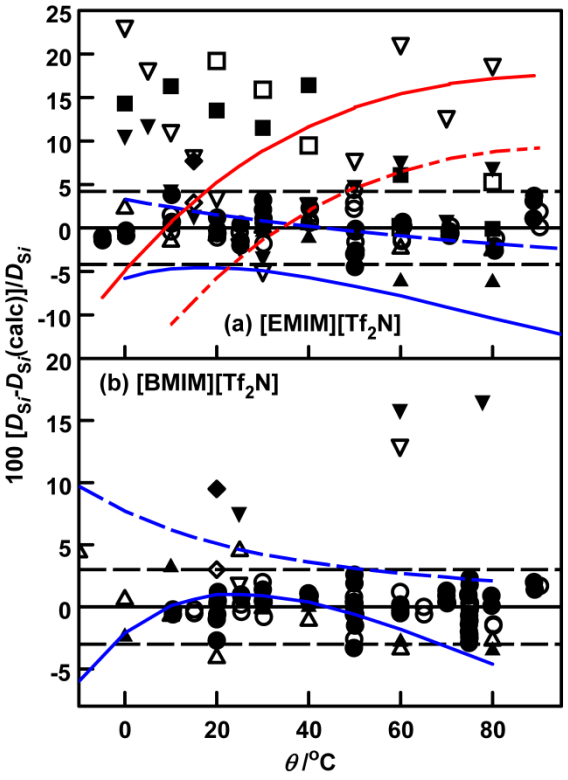

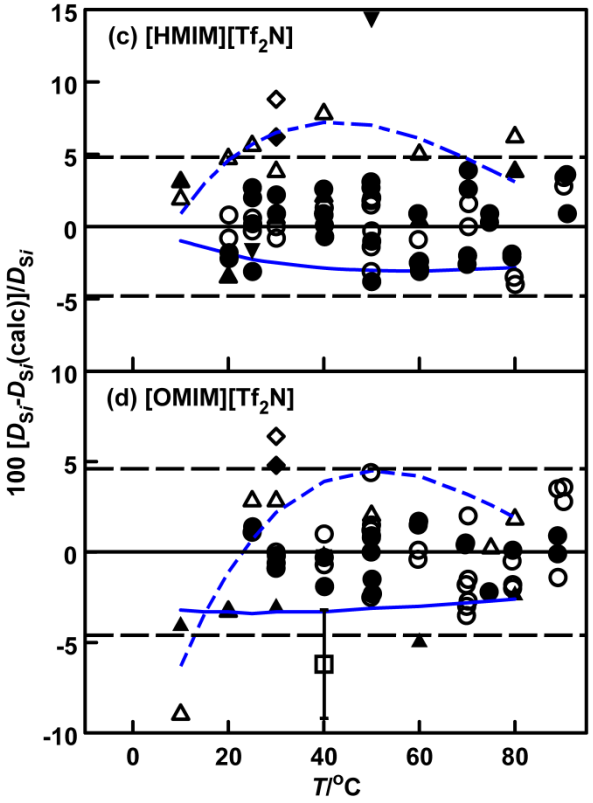

Fig. 4 Relative deviations for the fit of the atmospheric pressure self-diffusion coefficients (D_{Si}) to eqn (17) as a function of temperature: closed symbols, cation, D_{S+}; open symbols, anion, D_{S-}; a) [EMIM][Tf_2N]: circles, this work, the dotted lines show the expanded uncertainty with a 95% confidence level (k = 2), for the cation, U_r = 4.2%, for the anion U_r = 2.6%; squares, Noda et al.,[67] precision not given; triangles, Tokuda et al.,[40,68] precision not given data reported in ref. 40 as smoothed eq. and shown as blue lines in the Figures (cation, continuous; anion, dashed) are listed in the SI of ref. 68]; inverted triangles, Hayamizu et al.,[69] precision not given; diamonds, Martinelli et al.,[73] precision not given; red lines, smoothed eq., Borodin et al.,[72] relative standard uncertainty u_r = 5%. b) [BMIM][Tf_2N]: circles, this work, the dotted lines show the expanded uncertainty with a 95% confidence level for both ions (k = 2), U_r = 3%; triangles, Tokuda et al.,[40,68-71] (data reported in ref. 40, 70 and 71 are listed in the SI of ref. 68; the line represents the fit given in ref. 40 for the anion but lies above the points listed); inverted triangles, Hazelbaker et al.,[74] u_r = 8-10%; diamonds, Martinelli et al.[73]; the data of Chiappe et al.[75] lie off-scale. (c) [HMIM][Tf_2N]: circles, this work, the dotted lines show the expanded uncertainty with a 95% confidence level (k = 2) for the cation, U_r = 3.6%, for the anion U_r = 2.8%; triangles, Tokuda et al.,[40,68] (the line represents the fit given in ref. 40 for the cation and lies below the points listed in ref. 62); diamonds, Martinelli et al.[73] (d) [OMIM][Tf_2N]: circles, this work, the dotted lines show the expanded uncertainty with a 95% confidence level (k = 2) for the anion, U_r = 3%, for the cation U_r = 2.6%; squares, Umecky et al., u_r = 3% (error bar shown for D_{S-});[65] triangles, Tokuda et al.;[40,68] diamonds, Martinelli et al.[73]

$$D_{Si} = \exp[a + bp + (c + dp + ep^2)/(T - T_0)], \quad i = +, - \qquad (19)$$

and MVFT2, with T_0 a function of p) employed in earlier studies at high pressure:[1-3]

$$D_{Si} = \exp\{a + bp + \delta(x + yp + zp^2)/[T - (x + yp + zp^2]\}, \quad i = +, - \qquad (20).$$

Table 5 Coefficients for the VFT equation, (17), for the Ionic Self-diffusion Coefficients of [EMIM][Tf_2N], [BMIM][Tf_2N], [HMIM][Tf_2N] and [OMIM][Tf_2N] at 0.1MPa.

	[EMIM][Tf_2N]		[BMIM][Tf_2N]	
	D_{S+}	D_{S-}	D_{S+}	D_{S-}
A [a]	10.102 (0.16)	9.209 (0.20)	10.089 (0.17)	9.442 (0.13)
$-B$ /K	1045.8 (58)	875.2 (67)	1083.4 (62)	920.34 (41)
T_0 /K	128.00 (4.9)	146.85 (6.4)	138.36 (5.0)	154.32 (3.6)
u_r /% [b]	2.1	1.8	1.5	1.0
T range /°C	-5 - 89	10 - 80	10 - 89	15 - 90
	[HMIM][Tf_2N]		[OMIM][Tf_2N]	
	D_{S+}	D_{S-}	D_{S+}	D_{S-}
A [a]	9.470 (0.29)	10.913 (0.41)	9.470 (0.29)	10.913 (0.41)
$-B$ /K	905.12 (95)	1449.4 (166)	905.12 (95)	1449.4 (166)
T_0 /K	161.41 (8.3)	122.13 (11)	161.41 (8.3)	122.13 (11)
u_r /% [b]	2.4	2.1	2.4	2.1
T range /°C	20 - 91	20 - 90	20 - 91	20 - 90

[a] The standard errors for the fitted coefficients are given in parentheses. D_{Si} units: $10^{-12}m^2 \cdot s^{-1}$. [b] u_r, relative standard uncertainty of the fit.

Table 6 Coefficients for the modified VFT (MVFT1 and MVFT2) equations, (19) and (20) for the Ionic Self-diffusion Coefficients of [BMIM][Tf_2N]

	MVFT1			MVFT2	
	D_{S+}	D_{S-}		D_{S+}	D_{S-}
a [a]	10.028 (0.13)	9.627 (0.19)	a	9.8746 (0.13)	9.7234 (0.20)
b / 10^{-3} MPa^{-1}	2.587 (0.47)	3.939 (0.78)	b / 10^{-3} MPa^{-1}	-1.006 (0.31)	-1.523 (0.53)
c /K	-1060.9 (47)	-980.2 (65)	δ	-6.952 (0.48)	-6.931 (0.75)
d / $K \cdot MPa^{-1}$	-2.110 (0.10)	-2.362 (0.16)	x / K	144.84 (3.8)	146.31 (5.8)
e / 10^{-3} $K \cdot MPa^{-2}$	0.6647 (0.076)	1.0489 (0.11)	y / $K \cdot MPa^{-1}$	0.1098 (0.046)	0.1309 (0.083)
T_0/K	140.30 (3.9)	149.20 (5.6)	z / 10^{-6} $K \cdot MPa^{-2}$	-88.54 (5.4)	-133.9 (15)
u_r /% [b]	1.5	1.7	u_r /% [b]	1.5	1.8

[a] The standard errors for the fitted coefficients are given in parentheses. D_{Si} units: $10^{-12}m^2 \cdot s^{-1}$. [b] u_r, relative standard uncertainty of the fit.

The fitting parameters for eqn (17), (19) and (20) are given in Tables 5 and 6.

Fig. 4 shows deviation plots for the fits of the atmospheric pressure ion self-diffusion coefficients to the VFT equation, (17), and a comparison with literature results. Pulsed field gradient NMR data from the Sendai laboratory for [OMIM][Tf_2N] at 40 °C agree well with the steady gradient results reported here.[65] For [EMIM][Tf_2N], there are several sets of data measured by Hayamizu[66] and her colleagues in the period 2000 to 2011 using both synthesized[40,67,68] and commercial samples.[69] Fig. 4(a) shows that the 2005

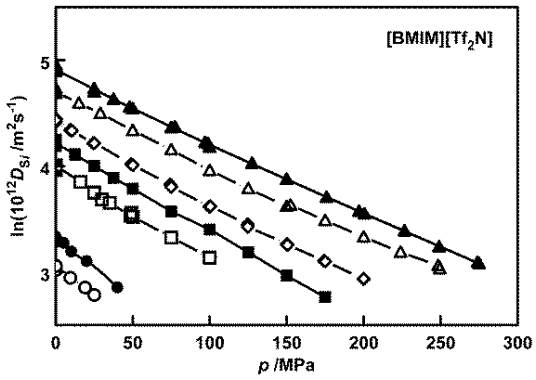

Fig. 5 Pressure dependence of the self-diffusion coefficients of [BMIM][Tf_2N]: closed symbols, cation, D_{S+}; open symbols, anion, D_{S-}; circles, 25 °C; squares, 50 °C; diamonds, 65 °C; triangles, 75 °C.

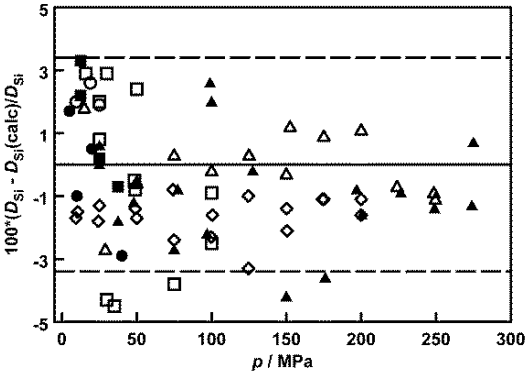

Fig. 6 Relative deviations for the fit of the high-pressure self-diffusion coefficients (D_{Si}) for [BMIM][Tf_2N] to eqn (19) (MVFT1) as a function of pressure: symbols, as Fig. 5. The dotted lines show the expanded uncertainty with a 95% confidence level (k = 2) for the cation $\underline{u}_r$ = 4%, for the anion u_r = 3.2%.

measurements of Tokuda et al.[40] (triangles, data listed in the SI for ref. 68) best agree with the results of this work, but those from ref. 67 and 69 appear to be too high. The data of Tokuda et al.[40] for the other three ILs [Fig. 4(b) to (d)] are also best agreement with our results. (Note that the data from ref. 40 for [BMIM][Tf_2N] reappear in related papers[70,71]). The measurements of Borodin et al.[72] [EMIM][Tf_2N], there are several sets of data measured by have a much steeper temperature dependence than either our values or those of Tokuda et al.,[40] with self-diffusion coefficients for the cation at high temperatures and for the anion at low temperatures well outside the bounds of the stated experimental uncertainty. The values of Martinelli et al.[73] at 30 °C for [EMIM][Tf_2N] lie (8 and 3) % above our work for the cation and anion respectively; for [BMIM][Tf_2N] the deviations are (7 and 3) %, for [HMIM][Tf_2N] (6 and 8) % and for [OMIM][Tf_2N] (5 and 7) %, so their self-diffusion coefficients are consistently higher

than our results for this series of salts by about 6%. For [BMIM][Tf_2N], the results of Hazelbaker et al.[74] are generally 9 to 24 % higher than ours, with only the datum for the anion at 25 °C in good agreement; the results of Chiappe et al.[75] at 32 °C are some 25% higher than those of this work. For [HMIM][Tf_2N], the result of Ahosseini et al.[56] for the cation at 25 °C agrees fairly well, but that at 50 °C is 14% higher that of this work. These high results are very likely due to water contamination which can have a large effect on the transport properties of ionic liquids. In our experience it is necessary to dry glass NMR tubes by evacuation while heating with a gas flame. Our high-pressure diffusion cell is constructed of hydrophobic PFTE which also reduces the likelihood of contamination.

Fig. 5 shows the pressure dependence of the self-diffusion coefficients of [BMIM][Tf_2N]. The approximately exponential decrease with increasing pressure is typical of un-associated liquids. Fig. 6 is the deviation plot for the fit of the ion self-diffusion coefficient isotherms to the modified VFT equation, (19), excluding atmospheric pressure points for clarity. There are no published high pressure measurements for comparison.

Fig. 7(a) shows the ratio D_+/D_- as a function of temperature for all the salts at atmospheric pressure: the error bars are based on the uncertainty estimate of 3% for the self-diffusion coefficients. In each case the ratio is greater than unity, and is the larger the smaller the cation. These values may be compared with those for tetrafluoroborate and hexafluorophosphate salts of the same cations in Fig. 7(b). The ordering in terms of the cation is the same as for the $[Tf_2N]^-$ salts, but values smaller than unity obtain for the salts of the larger cations.

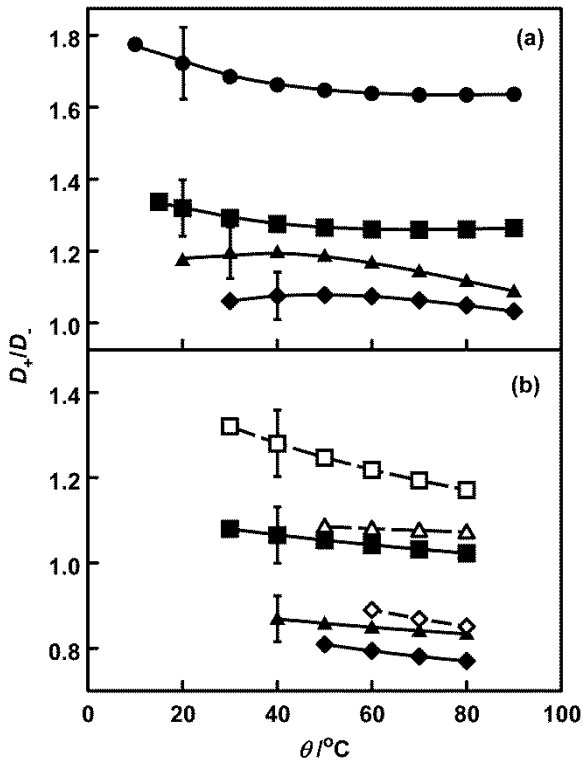

Fig. 7 Cation-anion self-diffusion coefficient ratios at atmospheric pressure for (a) $[Tf_2N]^-$ salts (this work) and (b) $[BF_4]^-$ salts,[2] closed symbols, and $[PF_6]^-$ salts,[1,2] open symbols. $[EMIM]^+$, circles; $[BMIM]^+$, squares; triangles, $[HMIM]^+$; diamonds, $[OMIM]^+$. See also Table 2 of ref. 4. The error bars are based on a relative standard uncertainty of 3% in the self-diffusion coefficients.

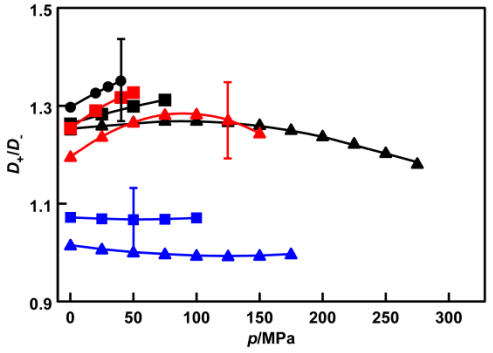

Fig. 8 Cation-anion self-diffusion coefficient ratios as a function of pressure, p, for 1-butyl-3-methylimidazolium salts: black symbols, [BMIM][Tf_2N]; red symbols, [BMIM][PF_6];[1] blue symbols, [BMIM][BF_4].[2] Symbols: circles, 25 °C; $[BMIM]^+$, squares, 50 °C; triangles, 75 °C. See also Fig. 3 of ref. 4. The error bars are based on a relative standard uncertainty of 3% in the self-diffusion coefficients.

Fig. 8 shows self-diffusion coefficient ratio as a function of pressure for [BMIM][Tf_2N] together with values for other [BMIM] salts. There are suggestions of small maxima in the longer isotherms (based on the MVFT1 smoothed fits), but these lie within the experimental uncertainty.

Discussion

As in our earlier studies of ionic liquid transport properties we again employ viscosity scaling relations for the conductivities and self-diffusion coefficients, and velocity correlation and distinct diffusion coefficients computed from these, which are linked through the Nernst-Einstein equation. We examine Laity resistance coefficients as an alternative to velocity correlation and distinct diffusion coefficients. Finally we correlate the high pressure data for [BMIM][Tf_2N] as functions of temperature and volume using thermodynamic scaling.

Empirical Viscosity Scaling Relationships

Fig. 9 and 10 show Stokes-Einstein-Sutherland and Walden plots for the self-diffusion coefficients and molar conductivities respectively. Very similar slopes (Table 7) are found for the plots for a given ionic liquid, in accord with our earlier studies on ionic liquids,[1-4,76,77] though it has to be remembered that this is an empirical correlation.[11] The high-pressure isotherms and the atmospheric pressure isobar data for [BMIM][Tf_2N] are overlaid as found in our previous high-pressure work.[1-4] It is curious that the SES plots for the anions in the [RMIM][Tf_2N] series very nearly overlie one another, whereas those for the

Table 7 Exponents (t) for Stokes-Einstein-Sutherland and Walden fits (Fig. 9 and 10) of the Self-diffusion coefficients, D_{Si}, Molar Conductivity Λ and Distinct Diffusion Coefficients, D^{d}_{ij} (Fig. 12) and the consistency test plot of ln(ΛT) against ln ($D_{S+} + D_{S-}$) (Fig. 11).

substance	$t(D_{S+})$	$t(D_{S-})$	$t(\Lambda)$	ln(ΛT) vs. ln ($D_{S+} + D_{S-}$)	$t(D^{d}_{++})$	$t(D^{d}_{--})$	$t(D^{d}_{+-})$
[EMIM][Tf_2N]	0.92_3	0.97_1	0.89_9	0.95_4	0.96_0	0.98_5	0.89_9
[BMIM][Tf_2N]	0.92_7	0.95_6	0.93_1	0.97_7	0.94_0	0.95_9	0.93_1
[HMIM][Tf_2N]	0.93_2	0.96_4	0.94_7	0.99_0	0.92_9	0.97_0	0.94_7
[OMIM][Tf_2N]	0.95_6	0.96_3	0.95_6	0.98_6	0.95_3	0.96_5	0.95_6

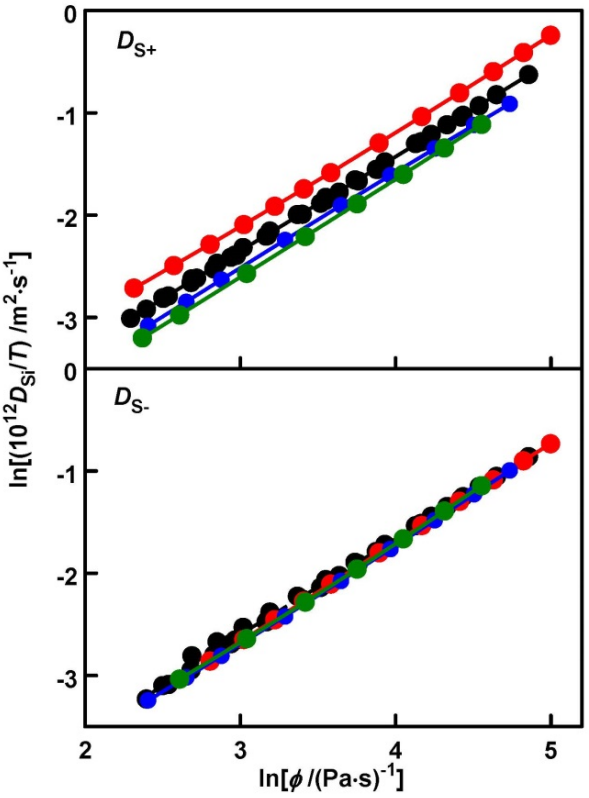

Fig. 9 Stokes-Einstein-Sutherland plots of self-diffusion coefficients, D_{Si}, against fluidity, ϕ (reciprocal viscosity) for [RMIM][Tf_2N] salts. Symbols: red, $[EMIM]^+$, atm p; black, $[BMIM]^+$, atm p and high p; blue, $[HMIM]^+$, atm p; green, $[OMIM]^+$, atm p; slopes: $[EMIM]^+$, 0.92_4 and 0.97_1; $[BMIM]^+$, 0.92_6 and 0.94_6; $[HMIM]^+$, 0.93_6 and 0.96_0; $[OMIM]^+$, 0.95_6 and 0.96_3, for D_{S+} and D_{S-} respectively.

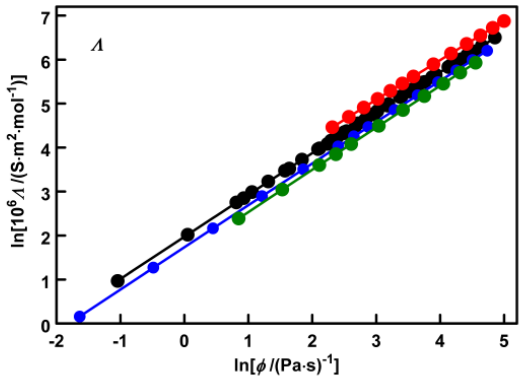

Fig. 10 Walden plots of molar conductivity, Λ, against fluidity, ϕ, (reciprocal viscosity) for [RMIM][Tf_2N] salts. Symbols: as in Fig. 9; slopes: $[EMIM]^+$, 0.89_9; $[BMIM]^+$, 0.93_0; $[HMIM]^+$, 0.94_0; $[OMIM]^+$, 0.95_6.

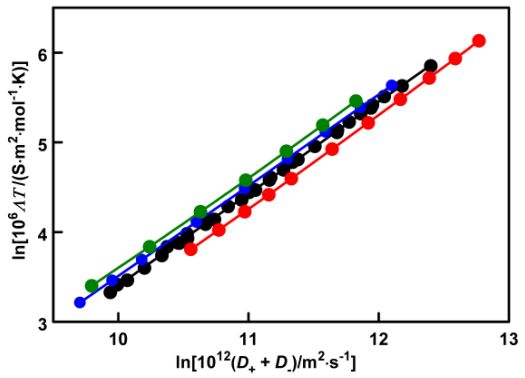

Fig. 11 Plots of ln($T\Lambda$) against ln($D_{S+} + D_{S-}$) for [RMIM][Tf_2N] salts. Symbols: as in Fig. 9; slopes: $[EMIM]^+$, 0.95_3; $[BMIM]^+$, 0.97_7; $[HMIM]^+$, 0.99_0; $[OMIM]^+$, 0.99_2

cations and for the conductivities in the Walden plots follow the order $[EMIM]^+ > [BMIM]^+ > [HMIM]^+ > [OMIM]^+$. Similar overlap was noted for $[Tf_2N]^-$ salts of the cations N-butyl-N-methylpyrrolidinium, $[Pyr_{14}]^+$, 1-ethyl-1,4-dimethylpiperazinium, $[C_2dmppz]^+$, and its open chain analogue, 1-(2-dimethylaminoethyl) dimethylethylammonium, $[C_2TMEDA]^+$.[76] The SES plots for these cations overlie those of the large $[OMIM]^+$ ion and the anion SES plots overlie those for the $[RMIM]^+$ series, (but are not shown in the figures as these would become too cluttered). Thus viscosity scaling much reduces the differences experimentally observed between the self-diffusion coefficients and conductivities in these ionic liquids.

We note that plots of ln(ΛT) versus ln($D_{S+} + D_{S-}$) are also linear with slopes very close to unity, as shown in Fig. 11 and Table 7; this is a test of the consistency of the experimental results, [1,2] as is implied by the Nernst-Einstein equation, (4), if Λ is a constant, independent of temperature and pressure (see below).

Finally we note that our lowest measured self-diffusion coefficient for [BMIM][Tf_2N] is of the order of $13 \cdot 10^{-12} \cdot m^2 \cdot s^{-1}$ so this lies above the region where dynamic crossover has been suggested.[78]

Velocity Cross-correlation Coefficients and Distinct Diffusion Coefficients

The velocity correlation (f_{ij}) and distinct diffusion coefficients calculated from the smoothed transport properties for each salt using eqn (1) to (3) are given in Table S7. As is always the case for ionic liquids, the cation-anion VCC are smallest in magnitude and least negative. In addition, as has been found to be the case for all the [Tf_2N]$^-$ salts we have studied thus far,[3,4,76,77] the cation-cation VCC is smaller in magnitude and less negative than the anion-anion VCC. The opposite is the case for 1-methyl-3-alkylimidazolium salts of the smaller and more symmetric [BF_4]$^-$ and [PF_6]$^-$ ions,[1,2,4] so there appears to be an anion effect.

Kashyap et al.[79] have pointed out that the VCC in single-component molten salts represent *anti-correlations* of the ensemble averaged ion velocities. These are a consequence of the requirement that momentum be conserved[79,80] and consequently there is not the possibility of the correlations seen in electrolyte solutions between oppositely charged ions[81,82] as there is no solvent or second component, only the two ion species, but it is to be expected that the cation-anion VCC is smaller in magnitude than either the cation-cation or anion-anion VCC due to the opposite charges of the ions. The different order for these last two quantities for [Tf_2N]$^-$ salts on the one hand and [BF_4]$^-$ and [PF_6]$^-$ salts on the other, as for the VCC, has yet to be explained, though it could be due to greater cation-cation contact when the anions are small as suggested by the molecular dynamics simulations of Klähn and Seduraman.[83] Linear and angular momentum exchange through translational-rotational coupling and caging of the smaller ions are other effects to be considered.

Examination of atmospheric pressure data in the literature for salts of anions intermediate in size to [BF_4]$^-$ and [PF_6]$^-$ on the one hand and [Tf_2N]$^-$ on the other, such as [$(FSO_2)_2N$]$^-$, [CF_3SO_4]$^-$ and [CH_3SO_4]$^-$, show apparent inconsistencies (e.g. markedly different slopes for SES and Walden plots and plots of $\ln(\Lambda T)$ versus $\ln[D_{S+} + D_{S+}]$ with $t << 1$, c.f. Fig. 11), so, regrettably, it is not yet possible to make meaningful comparisons with such salts.

Fig. 12 shows the distinct diffusion coefficients (as $-D^d_{ij}$, as, like the VCC, these quantities are negative – see eqn (3)) plotted against the fluidity in a Stokes-Einstein-Sutherland plot. In this case the cation-cation plots for the four [RMIM][Tf_2N] salts overlap as do those for the anion-anion DDC. (It should be noted that the log-log SES and Walden plots reduce small differences, so the overlaps, while close, are not exact super-positions.) There is a greater spread in the cation-anion VCC, reflecting the same differences seen in the Walden plot, Fig. 10 (n.b. $f_{+-} \propto D^d_{+-} \propto \Lambda$); however the slopes, t, are very similar for a given ionic liquid (Table 7). Fig. 13 shows DDC for the [RMIM][Tf_2N] salts at 298.15 K and 0.1 MPa as a function of the alkyl chain carbon number, n. Clearly $D^d_{+-} > D^d_{++} > D^d_{--}$, and the magnitude, and therefore the strength of the anti-correlation effect, decreases with increasing n, under these isothermal, isobaric conditions. The DDC become *more*

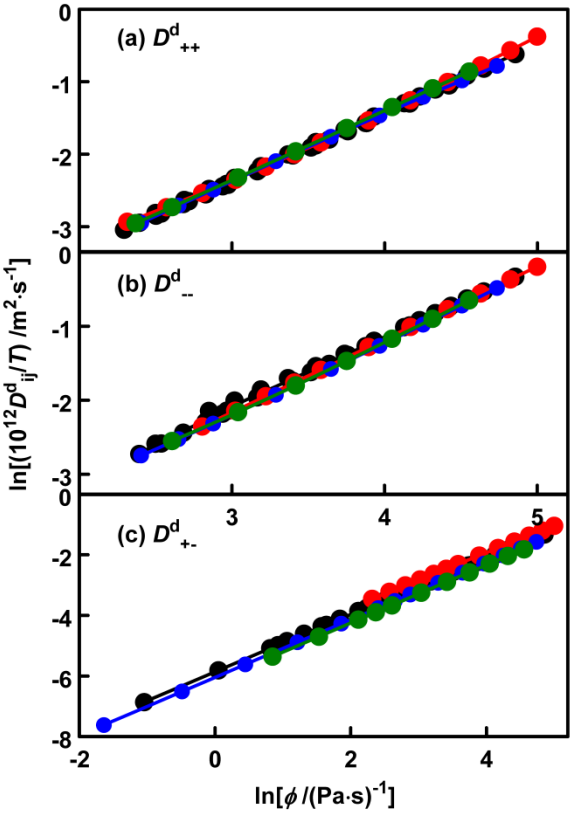

Fig. 12 Stokes-Einstein-Sutherland plots for the distinct diffusion coefficients for [RMIM][Tf_2N] salts. ϕ is the fluidity (reciprocal viscosity). Symbols as in Fig. 9. Note the difference between the scale of the x axis for the upper two panels and the lowest.

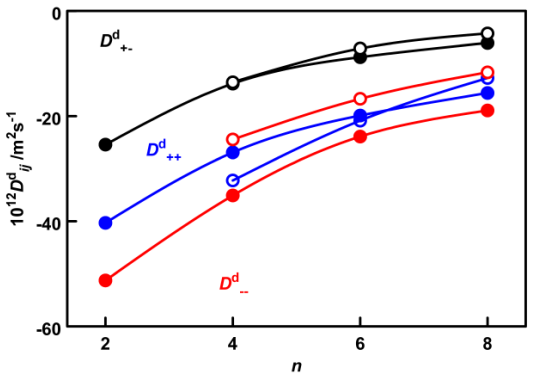

Fig. 13 Distinct diffusion coefficients for [RMIM][Tf_2N] salts (filled symbols) at 25 °C and 0.1 MPa compared with those for [RMIM][PF_6] salts at 50°C and 0.1 MPa (open symbols). n is the number of carbon atoms in the alkyl chain of the [RMIM]$^+$ cation. Symbols: black, cation-anion; blue, cation-cation; red, anion-anion. Note the different order for D^d_{++} and D^d_{--} for the two series: c.f. Fig. 2 of ref. 4.

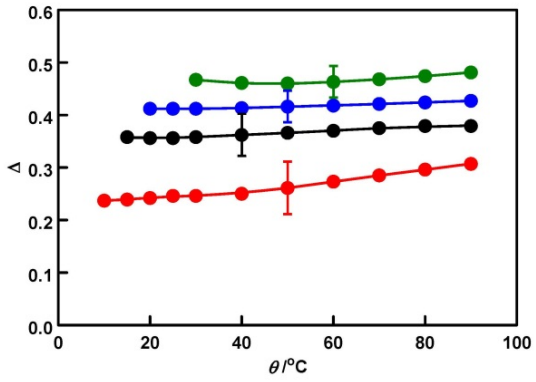

Fig. 14 Nernst-Einstein deviation parameter Δ for [RMIM][Tf_2N] as a function of temperature at 0.1 MPa. Symbols as in Fig. 9.

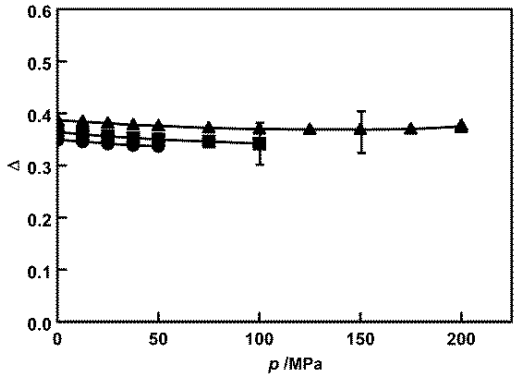

Fig. 15 Nernst-Einstein deviation parameter Δ for [BMIM][Tf_2N] as a function of pressure, p. Symbols: circles, 25 °C; squares, 50 °C; triangles, 75 °C.

negative with increasing temperature and *less* negative with increasing pressure (Table S7). However, Fig. 12 shows that the viscosity is really the controlling parameter for this series of salts, an increase of viscosity with decreasing temperature or increasing pressure leading to less negative DDC.

Nernst-Einstein Equation

Nernst-Einstein deviation parameters, Δ, calculated using eqn (4), are given in Table S7 and shown as a function of temperature at atmospheric pressure in Fig. 14 and, for [BMIM][Tf_2N], as a function of pressure in Fig. 15. Within experimental standard uncertainty (0.03 to 0.5, see Table S7), Δ *is* independent of temperature, though there is a suggestion of a mild temperature dependence for [EMIM][Tf_2N], consistent with the smaller slope (0.95) in the plot of $\ln(\Lambda T)$ versus $\ln(D_{S+} + D_{S-})$ for this salt. Δ is independent of pressure between 25 and 75 °C, as found previously for the $[BF_4]^-$ and $[PF_6]^-$ salts of $[RMIM]^+$ cations,[1,2] and for [Pyr_{14}] [Tf_2N].[3]

Δ increases significantly in magnitude in the series [EMIM][Tf_2N] to [OMIM][Tf_2N] as the alkyl group is lengthened. The same trend has been seen for the $[BF_4]^-$ and $[PF_6]^-$ salts.[2] As we have argued previously,[1,2,11] Δ does not straightforwardly describe the so-called "ionicity" (free ion – total ion ratio), but the reduction of the conductivity relative to the NE estimate due to the collective interactions of cations and anions with one another. This argument is supported by molecular dynamics simulations.[79,81] As is apparent in eqn 5, Δ is given by the difference between the cation-anion VCC and the mean of the cation-cation and anion-anion VCC. This is always non-zero, even for simple molten salts, as has been demonstrated by both molecular dynamics simulations (see ref. 12 of ref. 2 for a listing) and data for simple high-temperature molten salts.[1,84] One may speculate that this change in Δ is due to the "existence of a polar network formed by the charged moieties of the molecular ions" and "separations between different strands of the polar network caused by a continuous nonpolar sub-phase formed by the alkyl side chains that may be present in some of the ions" [85] as found in molecular simulations of $[RMIM]^+$ salts due to Canongia Lopes et al.,[83,86] and from small-wide angle X-ray scattering work, [87,88] but a direct link to the transport properties has yet to be

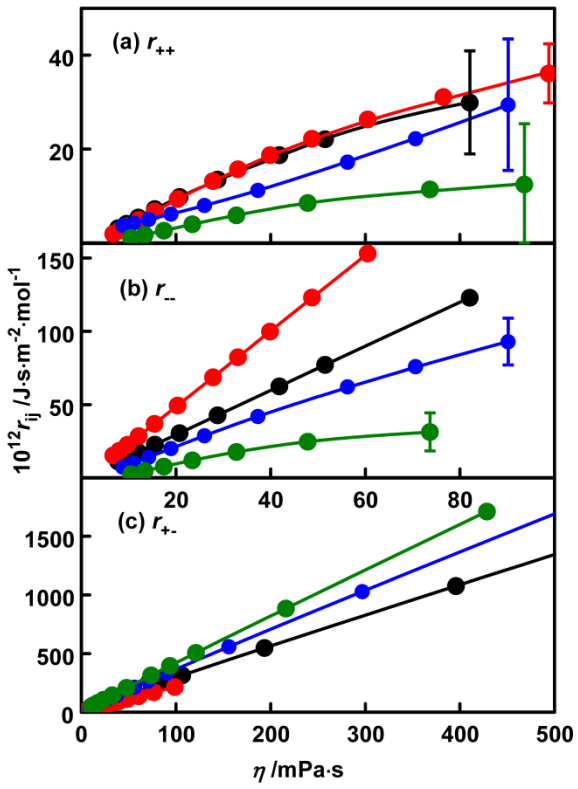

Fig. 16 Plots of the Laity resistance coefficients for [RMIM][Tf_2N] salts against the viscosity, η, at 0.1 MPa. Symbols as in Fig. 9. Note the difference between the scale of the x axis for the upper two panels and the lowest and between the three y axes. The errors are not constant, but decrease with deceasing viscosity for r_{++} and r_{--}, and from [OMIM][Tf_2N] (lowest D_{si} and Λ) to [EMIM][Tf_2N] (highest D_{si} and Λ).

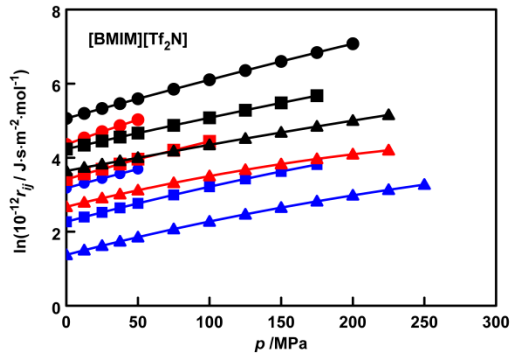

Fig. 17 Laity resistance coefficients r_{ij} for [BMIM][Tf_2N] as a function of pressure, p. Symbols: black, r_{+-}; blue, r_{++} ; red, r_{--}; circles, 25 °C; squares, 50 °C; triangles, 75 °C.

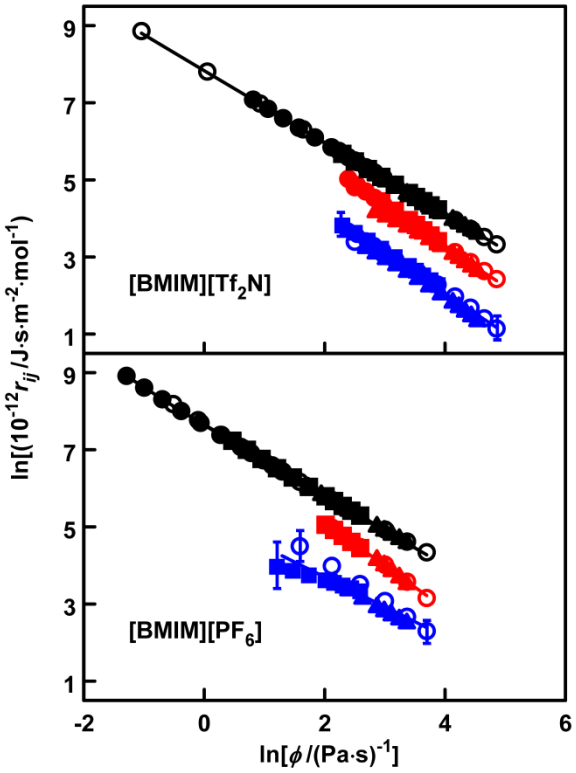

Fig. 18 Laity resistance coefficients r_{ij} for [BMIM][Tf_2N] and [BMIM][PF_6] as a function of fluidity, ϕ, (reciprocal viscosity). Symbols: black, r_{+-}; blue, r_{++} ; red, r_{--}; open circles, 0.1 MPa; filled circles, 25 °C; filled squares, 50 °C; filled triangles, [BMIM][Tf_2N] at 75 °C and [BMIM][PF_6] at 70 °C.

demonstrated.

Frictional Coefficients

The Laity resistance coefficients (LRC) calculated from (8) and (9) are also listed in Table S7. Fig. 16 shows the atmospheric pressure values as a function of viscosity – they increase with increasing viscosity as one would expect by analogy to the simple, hydrodynamic Stokes relation between a frictional coefficient and the viscosity. Fig. 17 shows the dependence on pressure for [BMIM][Tf_2N]; again the near-exponential increase with increase in pressure follows that for the viscosity.

Fig. 18 is an analogue of an SES plot for [BMIM][Tf_2N], with a corresponding plot for [BMIM][PF_6], based on data from ref. 1, for comparison. Fig. S1 is another SES analogue plot for all the systems at 0.1MPa. Note the larger uncertainties for the smaller r_{++} and r_{--}, which are the difference between two larger terms of similar size. (The VCCs are also the sum of a positive and a negative term, but the first is usually about half the magnitude of the second, so the relative uncertainties are less for VCC than LRC). The plot for the r_{+-} is yet another version of a Walden plot (see eqn. 8). The plots for the cation-cation and anion-anion resistance coefficients appear to be linear, but the uncertainty is larger than for the cation-anion, particularly for the former due to their smallness, than in the corresponding distinct diffusion coefficient plots.

The LRC are in the order $r_{+-} >> r_{--} >> r_{++}$ for all four $[Tf_2N]^-$ salts, with $r_{+-}^2 >> (r_{++}\, r_{--})$, in accord with $\Delta < 1$. The smallness of the cation r_{++} relative to that of the anion r_{--} is noteworthy given the large variation observed in (D_+/D_-) ratios shown in Fig. 7: this is difficult to interpret at this stage, though the larger r_{--} appears to correlate with the larger magnitude of D^d_{--}. A comparison with molten salts will be made in a separate publication.

Thermodynamic Scaling

As mentioned in the Introduction, it has been found that the transport properties of both molecular and ionic liquids can be scaled in terms of the group (TV^γ). As in our earlier work,[3] we use the simplest option of scaling by fitting ln P (where P is the relevant transport property) to simple polynomials in (TV^γ), choosing γ such that the isotherms fall on a common curve with minimized residuals. For [BMIM][Tf_2N] there were good fits within the experimental uncertainty of 3%, (D_{S+}: 1.7%, D_{S-}: 1.9), over the self-diffusion data sets, with the exception of the 75 °C isotherm for D_{S-} where there were slightly high deviations (more than twice the uncertainty) at some intermediate pressures. This was also the case for the conductivity at the highest pressures, but overall, a reasonably good fit was obtained (Λ: 1.8%).[‡] Given the simplicity of the approach and that there is only one disposable parameter, the quality and utility of the model are quite good. Earlier estimates for γ for the viscosity and self-diffusion coefficients of [BMIM][Tf_2N] were given by López et al.[9]

The scaling results for all the transport properties are listed in Table 8. It is found that the γ values for the reduced electrical and molar conductivities, viscosity and self-diffusion coefficients for [BMIM][Tf_2N] all lie very close together, appearing to confirm the Fragiadakis-Roland approach for molecular liquids and suggesting that all the reduced transport properties for ionic liquids scale similarly with the temperature and the density.

Table 8 also lists scaling results calculated for the other ionic liquids where there exist high-pressure self-diffusion, viscosity and conductivity data. (Most of these systems were also examined in the thermodynamic scaling study of López et al.,[9] but the calculations have been revised with the use of newer high pressure *pVT* data for the imidazolium ILs, published since by Smith et al.[89,90]) Generally, these confirm the result obtained for [BMIM][Tf_2N], though there is some divergence with the more difficult to determine self-diffusion coefficients for the more viscous salts. The molecular dynamics studies of Ohtori et al.,[91] who have shown that the thermal conductivity of model liquids, including high-temperature molten salts, scale with packing fraction in addition to volume and temperature, suggest that the differences observed between the scaling parameters for different ionic liquids may be due to differences in packing fraction, and therefore be a result of differences in liquid structure. If so, this would be a subject of great interest.

Values for the scaling parameters for the reduced conductivities of higher temperature molten salts for which both high pressure conductivities and densities are available are also included in Table 8: these are similar in magnitude to those of the (room-temperature) ionic liquids.

We note that the γ values for the reduced viscosity and conductivities are lower than those of the unreduced properties, and higher for the reduced self-diffusion coefficients. As found in the earlier study,[9] the γ values generally increase as the size (volume) of the cation is decreased for salts with a common anion. However the inorganic nitrates show the opposite trend.

Combination of the reduced self-diffusion coefficient and viscosity expressions. eqn (12) and (14), gives a form similar to the classical Stokes-Einstein-Sutherland equation.

Table 8 Scaling Parameters γ for the Transport Properties of Ionic Liquids. [a,b]

	η	η^*	κ	κ^*	Λ	Λ^*	D_{S+}	D_{S+}^*	D_{S-}	D_{S-}^*	*pVT* data	Transport property data
[BMIM][Tf_2N]	3.07	**2.83**	2.90	**2.81**	3.01	**2.81**	2.66	**2.79**	2.57	**2.78**	ρ[5]	η,[6] κ,[7] D, this work.
u_r(fit)/%	1.9	1.6	1.8	1.8	1.8	1.8	1.7	1.6	1.9	2.1		
	2		2		2		3		3			
[BMIM][PF_6]	3.09	**2.92**	3.02	**2.99**	3.16	**2.99**	2.35	**2.43**	2.76	**2.88**	ρ[90]	η,[60] κ,[1] D,[1]
u_r(fit)/%	2.1	1.9	1.1	1.2	1.1	1.1	3.3	4.2	2.3	2.3		
u_r(expt)/% [c]	2		3		3		3		3			
[HMIM][PF_6]	2.54	**2.44**	2.39	**2.33**	2.55	**2.43**	2.22	**2.32**	2.18	**2.28**	ρ[89]	η,[6] κ,[2] D,[2]
u_r(fit)/%	1.4	1.1	2.2	2.3	2.3	2.2	2.7	1.7	2.6	2.6		
[OMIM][PF_6]	2.31	**2.18**	2.17	**2.16**	2.19	**2.18**	1.86	**1.91**	2.1	**2.17**	ρ[89]	η,[92] κ,[30] D,[2]
u_r(fit)/%	1.2	1.0	2.4	1.6	2.3	1.9	2.6	2.7	1.8	1.8		
[BMIM][BF_4]	2.83	**2.67**	2.53	**2.48**	2.78	**2.48**	2.63	**2.76**	2.30	**2.40**	ρ[90]	η,[36] κ,[2] D,[2]
u_r(fit)/%	1.2	0.9	1.8	1.9	3.1	1.9	1.7	1.3	2.7	2.7		
[OMIM][BF_4]	2.18	**2.06**	2.17	**2.14**	2.25	**2.14**	1.83	**2.10**	1.88	**1.94**	ρ[93]	η,[92] κ,[30] D,[2]
u_r(fit)/%	5.9	5.2	3.2	3.3	3.1	3.2	3.1	4.1	3.8	3.8		
[Pyr_{14}][Tf_2N]	3.00	**2.80**					3.10	**3.20**	3.00	**3.20**	ρ(lit.)[3]	η,[3] D,[3]
u_r(fit)/%	2.3	2.0					2.1	0.7	1.6	2.0		
[$N(C_4H_9)_4$][$B(C_4H_9)_4$]	2.43	**2.19**			2.65	**2.39**					ρ[94]	η,[93] κ,[95]
u_r(fit)/%	3.0	3.0			2.7	2.9						
u_r(expt)/% [c]					5	5						
[$N(C_4H_9)_4$][BF_4]					2.00	**1.95**					ρ[96]	κ[96]
u_r(fit)/%					0.4	0.3						
u_r(expt)/% [c]					0.1	0.1						
[$N(C_5H_{11})_4$][BF_4]					1.63	**1.49**					ρ[96]	κ[96]
u_r(fit)/%					0.4	0.3						
[$N(C_6H_{13})_4$][BF_4]					1.47	**1.35**					ρ[96]	κ[96]
u_r(fit)/%					1.0	1.0						
[$N(C_7H_{15})_4$][BF_4]					1.25	**1.21**					ρ[96]	κ[96]
u_r(fit)/%					2.7	2.9						
$NaNO_3$					1.72	**1.25**					ρ[97,98]	κ[99,100]
u_r(fit)/%					0.6	0.6						
u_r(expt)/% [c]					1	1						
KNO_3					5.50	**3.81**					ρ[101]	κ[99,100]
u_r(fit)/%					1.1	1.0						

[a] γ values for the un-reduced transport properties are taken from Table II in ref. 9, except for **[**Pyr_{14}][Tf_2N] (ref. 3) and the two nitrates (this work). [b] The uncertainties in γ determined in this work are 0.02 based on the minimization of u_r(fit). [c] The experimental uncertainties are the same in the subsequent rows.

$$D_{Si} * \eta * = \frac{D_{Si}\eta v^{1/3}}{k_B T} \quad (21)$$

For the simple SES hydrodynamic model, for a particle of diameter σ,

$$\frac{D_{Si}\eta\sigma}{k_B T} = \frac{1}{n\pi} \quad (22)$$

Therefore the fact that the product (D_{Si}* η*) is not constant and instead scales as a function of (TV^{γ}) with a single value of γ is consistent with the well-known viscosity, and hence density, dependence of the Stokes-Einstein number n.[11] n is related to the fractional SES exponent t:[11,13]

$$\ln n = \ln n_o + (t-1)\ln \eta \quad (23)$$

so the empirical application of the SES model with a fractional exponent t seems to be consistent with thermodynamic scaling.

A characteristic of thermodynamic scaling is that the scaling function is not known from theory and hence empirical treatments such as the fit of ln P to a polynomial in the group (TV^{γ}), as employed here, are necessary to obtain the scaling parameters. This means properties for different substances are fitted to different empirical functions. Fig. 19 illustrates differences and similarities between the fits for κ* and η* for the 1-alkyl-3-methylimidazolium ionic liquids. These are arbitrarily normalised, on both axes, on the values for 25 °C and 0.1 MPa [(1,0) on the graphs] for convenience of comparison. The dependence on (TV^{γ}) is seen to be least for [BMIM][Tf_2N] and greatest for [HMIM][PF_6], [OMIM][PF_6] and [OMIM][BF_4], with [BMIM][PF_6] and [BMIM][BF_4] lying between. One may speculate that suitable scaling of the molar volumes, as in hard sphere approaches, might allow the overlay of these curves on one another to give quasi-universal scaling: on the other hand, the different curves may reflect differences in liquid structure.

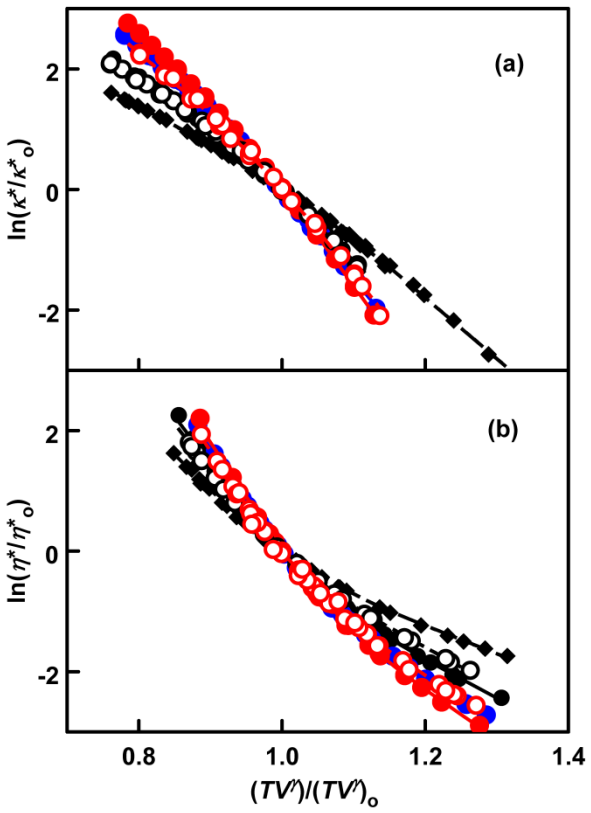

Fig. 19 Fits for the reduced electrical conductivities [κ*, panel (a)] and reduced viscosities [η*, panel (b)] for the [RMIM]$^+$ salts as a function of (TV)$^{\gamma}$. These are arbitrarily normalised, on both axes, on the respective values for 25 °C and 0.1 MPa [(1,0) on the graphs]. Symbols: diamonds, [BMIM][Tf_2N]; filled and open black circles, [BMIM][PF_6] and [BMIM][BF_4], respectively; filled blue circles, [HMIM][PF_6]; filled and open red circles, [OMIM][PF_6] and [OMIM][BF_4], respectively.

Conclusions

Ion self-diffusion coefficients have been measured for the ionic liquid 1-butyl-3-methylimidazolium bis(trifluoromethanesulfonyl)amide [BMIM][Tf_2N] at high pressure between 25 and 75 °C, supplemented by atmospheric pressure data between 10 and 90 °C. Together with previously published electrical conductivities and pVT measurements, the data are used to calculate velocity cross-correlation coefficients (VCC or f_{ij}) and distinct diffusion coefficients (D^d_{ij}). For comparison of trends within the 1-alkyl-3-methylimidazolium bis(trifluoromethanesulfonyl)amide series, self-diffusion coefficients, viscosities and electrical conductivities and densities are also reported for the 1-ethyl-, 1-hexyl- and 1-octyl-3-methylimidazolium bis(trifluoromethanesulfonyl)amide salts at atmospheric pressure.

Both the self-diffusion and distinct diffusion coefficients are analysed in terms of (fractional) Stokes-Einstein-Sutherland (SES) equations using viscosity data. The SES and Walden plots show almost identical slopes, with points for high-pressure isotherms and the atmospheric pressure isobar falling on common, single lines for each property for [BMIM][Tf_2N]. For the series [EMIM][Tf_2N] to [OMIM][Tf_2N], the anion SES plots overlap, whereas those for the cations and for the conductivities in the Walden plots follow the order [EMIM]$^+$ > [BMIM]$^+$ > [HMIM]$^+$ > [OMIM]$^+$.

Cation-anion self-diffusion coefficient ratios are found to be independent of temperature and pressure for [BMIM][Tf_2N], in accord with our earlier results for other ionic liquids. For the other [Tf_2N]$^-$ salts, the ratios are also found independent of temperature over the ranges experimentally accessible.

In common with other [Tf_2N]$^-$ salts, the velocity cross-correlation coefficients follow the order $f_{--} < f_{++} < f_{+-}$: our earlier work for [BF_4]$^-$ and [PF_6]$^-$ salts has shown the reverse order for the cation-cation and anion-anion f_{ij}, so these quantities appear to be more dependent on the nature of the anion, rather than that of the cation. The distinct diffusion coefficients (D^d_{ij} =

vcf_{ij}) for the [RMIM][Tf_2N] salts can be overlaid for both the cation-cation and anion-anion interactions, but there is more spread in the cation-anion case, mirroring the result of the Walden plot.

Laity resistance coefficients are calculated for ionic liquids for the first time. They also demonstrate SES behaviour, but the uncertainties are larger than for the distinct diffusion coefficients as the r_{++} and r_{--} are the resultant of two larger terms of similar size.

The Nernst-Einstein deviation parameter Δ for [BMIM][Tf_2N] appears to be independent of temperature. (between 10 and 90 ^oC) and pressure (below 200 MPa). Those for the other [Tf_2N]$^-$ salts are independent of temperature within experimental error. Δ increases in magnitude with increasing alkyl chain length on the cation.

The transport properties of [BMIM][Tf_2N] are re-examined in terms of density scaling as functions of the group (TV^γ) with reduced conductivities and reduced molar conductivities being calculated and scaled for the first time. In line with the examples of the scaling reduced self-diffusion coefficients and viscosities for molecular liquids reported by Fragiadakis and Roland[23] and López et al.,[9] the same scaling parameters (γ) are obtained for the viscosity, electrical conductivity, molar conductivity and both ion self-diffusion coefficients. This result is supported by the re-examination of data for other ionic liquids, suggesting that all the reduced transport properties for ionic liquids scale similarly with the temperature and the density. It is suggested that the γ for ionic liquids may depend on packing fraction.

Acknowledgements

We are grateful to Dr Lawrie Woolf (UNSW Canberra) for his interest in this work and to Ms Eriko Niitsuma (AIST, Sendai) for her assistance with some of the measurements. Dr Kikuko Hayamizu, University of Tsukuba, Japan, (formerly of AIST Tsukuba), generously provided details of her self-diffusion measurements, particularly for [EMIM][Tf_2N]. Emeritus Prof. Dr Klaus Tödheide (Karlsruhe, Germany) very kindly provided copies of his students' diplomarbeiten for data on molten salt conductivities. KRH acknowledges a travel grant from the (Australian) Prime Minister's Education Assistance Program for Japan in response to the Great East Japan Earthquake on 11 March 2011, in 2012, that assisted this work.

Notes and References

‡ We have attempted to scale the low-temperature (182 - 233 K), high-pressure (to 460 MPa) conductivity data of Wojnarowska et al.[38] for [BMIM][Tf_2N], obtaining $\gamma \sim 3.08$ for both κ and κ^* with relative standard uncertainties of fit of around 13%. This necessitated a considerable extrapolation of the equation of state used for the calculation of molar volumes so this result may not be reliable.

[1] M. Kanakubo, K. R. Harris, N. Tsuchihashi, K. Ibuki and M. Ueno, *J. Phys. Chem. B*, 2007, **111**, 2062.
[2] M. Kanakubo, K. R. Harris, N. Tsuchihashi, K. Ibuki and M. Ueno, *J. Phys. Chem. B*, 2008, **112**, 9830.
[3] K. R. Harris, L. A. Woolf, M. Kanakubo and T. Rüther, *J. Chem. Eng. Data*, 2011, **56**, 4672.
[4] K. R. Harris and M. Kanakubo, *Faraday Disc*., 2012, **154**, 425.
[5] M. Kanakubo and K. R. Harris, *J. Chem. Eng. Data*, 2015, **60**, 1408.
[6] K. R. Harris, M. Kanakubo and L. A. Woolf, *J. Chem. Eng. Data*, 2007, **52**, 1080.
[7] M. Kanakubo, K. R. Harris, N. Tsuchihashi, K. Ibuki and M. Ueno, *J. Chem. Eng. Data*, 2015, **60**, 1495.
[8] H. L. Friedman and R. Mills, *J. Sol. Chem.*, 1981, **10**, 395.
[9] E. R. López, A. S. Pensado, M. J. P. Comuñas, A. A. H. Pádua, J. Fernández and K. R. Harris, *J. Chem. Phys.*, 2011, **134**, 144507.
[10] H. Schönert, *J. Phys. Chem.*, 1984, **88**, 3359.
[11] K. R. Harris, *J. Phys. Chem. B*, 2010**, 114**, 9572.
[12] a) W. Nernst, *Z. Phys. Chem. (Leipzig)*, 1888, **2**, 613; b) W. Nernst, *Z. Phys. Chem. (Leipzig)*, 1889, **4**, 129; c) A. A. Noyes cited by R. Haskell, *Phys. Rev. (Series I)*, 1908, **27**, 145; d) G. S. Hartley, *Phil. Mag*., 1931, **12**, 473.
[13] H. J. V. Tyrrell and K. R. Harris, *Diffusion in Liquids*, Butterworths, London, 1984, Chapters 4.2 and 8.
[14] R. W. Laity, *J. Chem. Phys*., 1959, **30**, 682.
[15] R. W. Laity, *Ann. N. Y. Acad. Sci*., 1960, **79**, 997.
[16] L. Onsager, *Phys. Rev*., 1931, **37**, 405; 1931, **38**, 2265.
[17] R. Takagi and K. Kawamura, *Bull. Tokyo Inst. Tech*., 1975, **127**, 57.
[18] J. Fernández and E. R. López, Density Scaling Approach. In *Experimental Thermodynamics. Vol. IX. Advances in Transport Properties of Fluids*, ed. M. J. Assael, A. R. H. Goodwin, V. Vesovic and W. A. Wakeham, Royal Society of Chemistry, London, 2014, chapter 9.3.
[19] J. C. Dyre, *J. Phys. Chem. B*, 2014, **118**, 10007.
[20] T. B. Schrøder and J. C. Dyre, *J. Chem. Phys*., 2014, **141**, 204502.
[21] A. K. Bacher, T. B. Schrøder and J. C. Dyre, *Nat. Commun*., 2014, **5**, 5424.
[22] T. Schrøder, N. P. Bailey, U. R. Pedersen, N. Gnan and J. C. Dyre, *J. Chem. Phys.*, 2009, **131**, 23503.
[23] D. Fragiadakis and C. M. Roland, *J. Chem. Phys.*, 2011, **134**, 044504.
[24] Y. Rosenfeld, *J. Phys.: Condens. Matter*, 1999, **11**, 5415.
[25] S. Chapman and T. G. Cowling, *The Mathematical Theory of Non-Uniform Gases*, 2nd ed., Cambridge University Press, Cambridge, 1960, p. 359 ff.
[26] J. H. Dymond, *Chem. Soc. Rev.*, 1985, **14**, 317.
[27] R. J. Speedy, F. X. Prielmeier, T. Vardag, E. W. Lang and H.-D. Lüdemann, *Mol. Phys*., 1989, **66**, 577.
[28] K. R. Harris, *Mol. Phys.*, 1992, **77**, 1153.
[29] M. Kanakubo, H. Nanjo, T. Nishida and J. Takano, *Fluid Phase Equilib.*, 2011, **302**, 10.
[30] M. Kanakubo, K. R. Harris, N. Tsuchihashi, K. Ibuki and M. Ueno, *Fluid Phase Equilib.*, 2007, **261**, 414.

[31] R. L. Gardas, M. G. Freire, P. J. Carvalho, I. M. Marrucho, I. M. A. Fonseca, A. G. M. Ferreira, and J. A. P. Coutinho, *J. Chem. Eng. Data*, 2007, **52**, 1881.
[32] M. Tariq, P. A. S. Forte, M. F. Costa Gomes, J. N. Canongia Lopes and L. P. N. Rebelo, *J. Chem. Thermodynamics*, 2009, **41**, 790.
[33] C. Kolbeck, J. Lehmann, K. R. J. Lovelock, T. Cremer, N. Paape, P. Wasserscheid, A. P. Fröba, F. Maier and H.-P. Steinrück, *J. Phys. Chem. B*, 2010, **114**, 17025.
[34] J. Jacquemin, P. Nancarrow, D. W. Rooney, M. F. C. Gomes, A. A. H. Pádua and C. Hardacre, *J. Chem. Eng. Data*, 2008, **53**, 716-726.
[35] N. M. Yunus, M. I. Abdul Mutalib, Z. Man, M. Azmi Bustam and T. Murugesan, *J. Chem. Thermodynamics*, 2010, **42**, 491.
[36] K. R. Harris, M. Kanakubo and L. A. Woolf, *J. Chem. Eng. Data*, 2007, **52**, 2425.
[37] T. Makino, M. Kanakubo, Y. Masuda, T. Umecky and A. Suzuki, *Fluid Phase Equilib.*, 2014, **362**, 300.
[38] Z. Wojnarowska, G. Jarosz, A. Grzybowski, J. Pionteck, J. Jacquemin and M. Paluch, M. *Phys. Chem. Chem. Phys.*, 2014, **16**, 20444.
[39] J. A. Widegren, E. M. Saurer, K. N. Marsh and J. W. Magee, *J. Chem. Thermodynamics*, 2005, **37**, 569.
[40] H. Tokuda, K. Hayamizu, K. Ishii, M. Abu Bin Hasan Susan and M. Watanabe, *J. Phys. Chem. B*, 2005, **109**, 6103.
[41] J. A. Widegren and J. W. Magee, *J. Chem. Eng. Data*, 2007, **52**, 2331.
[42] M. E. Kandil, K. N. Marsh and A. R. H. Goodwin, *J. Chem. Eng. Data*, 2007, **52**, 2382.
[43] J. Leys, M. Wübbenhorst, C. P. Menon, R. Rajesh, J. Thoen, C. Glorieux, P. Nockemann, B. Thijs, K. Binnemans and S. Longuemart, *J. Chem. Phys.*, 2008, **128**, 064509.
[44] F. J. V. Santos, C. A. Nieto de Castro, P. J. F. Mota and A. P. C. Ribeiro, *Int. J. Thermophys.*, 2010, **31**, 1869.
[45] M. S. Calado,·J. C. F. Diogo, J. L. Correia da Mata Fernando, J. P. Caetano, Z. P. Visak and J. M. N. A. Fareleira, *Int. J. Thermophys.*, 2013, **34**, 1265.
[46] A. Rupp , N. Roznyatovskaya, H. Scherer, W Beichel, P. Klose, C. Sturm, A. Hoffmann, J. Tübke, T. Koslowski and I. Krossing, *Chem. - Eur. J.*, 2014, **20**, 9794.
[47]A. Nazet, S. Sokolov, T. Sonnleitner, T. Makino, M. Kanakubo and R. Buchner, *J. Chem. Eng. Data*, 2015, **60**, 2400.
[48] Y. Pan, L. E. Boyd, J. F. Kruplak, W. E. Cleland, J. S. Wilkes and C. L. Hussey, *J. Electrochem. Soc.*, 2010, **158**, F1.
[49] R. D. Chirico, V. Diky, J. W. Magee, M. Frenkell and K. N. Marsh, *Pure Appl. Chem.*, 2009, **81**, 791.
[50] M. Vranes, N. Zec, A. Tot, S. Papovic, S. Dozic and S. Gadzuric, *J. Chem. Thermodynamics*, 2014, **68**, 98.
[51] M. Atilhan, J. Jacquemin, D. Rooney, M. Khraisheh and S. Aparicio, *Ind. Eng. Chem. Res.*, 2013, **52**, 16774.
[52] J. Salgado, T. Regueira, L. Lugo, J. Vijande, J. Fernandez, J. Garcia, *J. Chem. Thermodynamics*, 2014, **70**, 101.
[53] J. C. F. Diogo. F. J. P. Caetano, J. M. N. A. Fareleira and W. A. Wakeham, *Fluid Phase Equilib.*, 2013, **353,** 76.
[54] Y. Hiraga, A. Kato, Y. Sato and R. L. Smith, Jr., *J. Chem. Eng. Data*, 2015, **60**, 876.
[55] M. Tariq, P. J. Carvalho, J. A. P. Coutinho, M. Marrucho, J. N. Canongia Lopes and L. P. N. Rebelo, *Fluid Phase Equilib.*, 2011, **301**, 22.
[56] A. Ahosseini, L. R. Weatherley and A. M. Scurto, *J. Chem. Eng. Data*, 2011, **56**, 3715.
[57] M. Iguchi, Y. Hiraga, Y. Sato, T. M. Aida, M. Watanabe and R. L. Smith, Jr, *J. Chem. Eng. Data*, 2014, **59**, 709.
[58] R. Salinas, J. Pla-Franco, E. Lladosa and J. B. Montón, *J. Chem. Eng. Data*, 2015, **60**, 525.
[59] D. Almantariotis, T. Gefflaut, A. A. H. Pádua, J.-Y. Coxam, and M. F. Costa Gomes, *J. Phys. Chem. B*, 2010, **114**, 3608.
[60] A. V. Blokhin, Y. U. Paulechka, A. A. Strechan and G. J. Kabo, *J. Phys. Chem. B*, 2008, **112**, 4357.
[61] A. V. Blokhin, Y. U. Paulechka and G. J. Kabo, *J. Chem. Eng. Data*, 2006, **51**, 1377.
[62] Y. U. Paulechka, A. V. Blokhin, G. J. Kabo and A. A. Strechan, *J. Chem. Thermodynamics*, 2007, **39**, 866.
[63] J. C. F. Diogo. F. J. P. Caetano,·J. M. N. A. Fareleira and W. A. Wakeham, *Int. J. Thermophys.*, 2014, **35**, 1615.
[64] K. R. Harris, L. A. Woolf and M. Kanakubo, *J. Chem. Eng. Data*, 2005, **50**, 1777.
[65] T. Umecky, K. Suga, E. Masaki, T. Takamuku, T. Makino, M. Kanakubo, *J. Mol. Liq.*, 2015, **209**, 557.
[66] K. Hayamizu, On Accurate Measurements of Diffusion Coefficients by PGSE NMR Methods (Version 2) -Room-Temperature Ionic Liquids**.** http://diffusion-nmr.jp/wordpress/wp-content/uploads/2015/02/On-accurate-measurements-2015-1-191.pdf, accessed 8 Mar 2015.
[67] A. Noda, K. Hayamizu, and M. Watanabe, *J. Phys. Chem. B*, 2001, **105**, 4603.
[68] H. Tokuda, S. Tsuzuki, M. Abu Bin Hasan Susan, K. Hayamizu, and M. Watanabe, *J. Phys. Chem. B*, 2006, **110,** 19593.
[69] K. Hayamizu, S. Tsuzuki, S. Seki and Y. Umebayashi, *J. Chem. Phys.*, 2011, **135**, 084505.
[70] H. Tokuda, K. Hayamizu, K. Ishii, M. Abu Bin Hasan Susan and M. Watanabe, *J. Phys. Chem. B*, 2004, **108**, 16593.
[71] H. Tokuda, K. Ishii, Md. Abu Bin Hasan Susan, S. Tsuzuki, K. Hayamizu and M. Watanabe, *J. Phys. Chem. B*, 2006, **110**, 2833.
[72] O. Borodin, W. Gorecki, G. D. Smith and M. Armand, *J. Phys. Chem. B*, 2010, **114**, 6786.
[73] A. Martinelli, M. Marechal, A. Oestlund and J. Cambedouzou, *Phys. Chem. Chem. Phys.*, 2013, **15**, 5510.
[74] E. D. Hazelbaker, S. Budhathoki, A. Katihar, J. K. Shah, E. J. Maginn and S. Vasenkov, *J. Phys. Chem. B*, 2012, **116**, 9141.
[75] C. Chiappe, A. Sanzone, D. Mendola, F. Castiglione, A. Famulari, G. Raos and A. Mele, *J. Phys. Chem. B*, 2013, **117**, 668.
[76] T. Rüther, K. R. Harris, M. D. Horne, M. Kanakubo, T. Rodopoulos, J.-P. Veder, and L. A. Woolf, *Chem. Eur. J*, 2013, **19**, 17733.
[77] K. R. Harris, T. Makino and M. Kanakubo, *Phys. Chem. Chem. Phys.*, 2014, **16,** 9161.
[78] A. O. Seyedlar, S. Stapf and C. Mattea, *Phys. Chem. Chem. Phys.*, 2015, **17,** 1653.

[79] H. K. Kashyap, H. V. R. Annapureddy, F. O. Raineri and C. J. Margulis, *J. Phys. Chem. B*, 2011, **115**, 13212.
[80] H.-G. Hertz, *Ber. Bunsenges. phys. Chem.*, 1977, **8**1, 656.
[81] H.-G. Hertz, K. R. Harris, L. A. Woolf and R. Mills, *Ber. Bunsenges. phys. Chem.*, 1977, **81**, 664.
[82] L. A. Woolf and K. R. Harris, *J. Chem. Soc., Faraday Trans. I*, 1978, **74**, 933; corrigendum, 1979, **75**, 2873.
[83] M. Klähn and A. Seduraman, *J. Phys. Chem. B*, 2015, **119**, 10066
[84] J. Trullàs and J. A. Padró, *Phys. Rev. B*, 1997, **55**, 12210.
[85] K. Shimizu and J. N. Canongia Lopes, *J. Mol. Liq.*, 2015, in press, DOI:10.1016/j.molliq.2015.04.014.
[86] C. E. S. Bernardes, K. Shimizu, A. I. M. C. Lobo Ferreira, L. M. N. B. F. Santos and J. N. Canongia Lopes, *J. Phys. Chem. B*, 2014, **118**, 6885.
[87] K. Fujii, R. Kanzaki, T. Takamuku, Y. Kameda, S. Kohara, M. Kanakubo, M. Shibayama, S. Ishiguro and Y. Umebayashi, *J. Chem. Phys.*, 2011, **135**, 244502.
[88] M. A. A. Rocha, C. M. S. S. Neves, M. G. Freire, O. Russina, A. Triolo, J. A. P. Coutinho and L. M. N. B. F. Santos, *J. Phys. Chem. B*, 2013, **117**, 10889.
[89] R. Taguchi, H. Machida, Y. Sato and R. L. Smith, Jr, *J. Chem. Eng. Data*, 2009**, 54**, 22.
[90] H. Machida, Y. Sato, R. L. Smith, Jr, *Fluid Phase Equilib.*, 2008, **264**, 147.
[91] N. Ohtori, Y. Ishii, Y. Togaa, T. Oono, and K. Takase, *Phys. Rev. E*, 2014, **89**, 022129.
[92] K. R. Harris, M. Kanakubo and L. A. Woolf, *J. Chem. Eng. Data*, 2006, **51**, 1161.
[93] Z. Gu and J. F. Brennecke, *J. Chem. Eng. Data*, 2002, **47**, 339.
[94] G. Morrison and J. E. Lind, Jr, *J. Chem. Phys.*, 1968, **49**, 5310.
[95] R. J. Speedy, *J. Chem. Soc., Faraday Trans. 1*, 1977, **73**, 471.
[96] A. F. M. Barton and R. J. Speedy, *J. Chem. Soc., Faraday Trans. 1*, 1974, **70**, 506.
[97] B. B. Owens, *J. Chem. Phys.*, 1966, **44**, 3918.
[98] J. E. Bannard and A. F. M. Barton, *J. Chem. Soc., Faraday Trans. 1***,** 1978, **74**, 153.
[99] A. Würflinger, Diplomarbeit, Universität Karlsruhe, Germany, 1970.
[100] A. S. Quist, A. Würflinger and K. Tödheide, *Ber. Bunsenges. phys. Chem*., 1972, **76**, 652.
[101] J. R. Christie, doctoral thesis, Kansas State University, USA, 1967.